

---

# Complex Momentum for Learning in Games

---

Jonathan Lorraine<sup>1,2</sup> David Acuna<sup>1,2,3</sup> Paul Vicol<sup>1,2</sup> David Duvenaud<sup>1,2</sup>

## Abstract

We generalize gradient descent with momentum for learning in differentiable games to have complex-valued momentum. We give theoretical motivation for our method by proving convergence on bilinear zero-sum games for simultaneous and alternating updates. Our method gives real-valued parameter updates, making it a drop-in replacement for standard optimizers. We empirically demonstrate that complex-valued momentum can improve convergence in adversarial games—like generative adversarial networks—by showing we can find better solutions with an almost identical computational cost. We also show a practical generalization to a complex-valued Adam variant, which we use to train BigGAN to better inception scores on CIFAR-10.

## 1. Introduction

Gradient-based optimization has been critical for the success of machine learning, updating a single set of parameters to minimize a single loss. A growing number of applications require learning in games, which generalize single-objective optimization. Common examples are GANs (Goodfellow et al., 2014), actor-critic models (Pfau & Vinyals, 2016), curriculum learning (Baker et al., 2019; Balduzzi et al., 2019; Sukhbaatar et al., 2018), hyperparameter optimization (Lorraine & Duvenaud, 2018; Lorraine et al., 2020; MacKay et al., 2019; Raghu et al., 2020), adversarial examples (Bose et al., 2020; Yuan et al., 2019), learning models (Rajeswaran et al., 2020; Abachi et al., 2020; Bacon et al., 2019), domain adversarial adaptation (Acuna et al., 2021), neural architecture search (Grathwohl et al., 2018; Adam & Lorraine, 2019), and meta-learning (Ren et al., 2018; 2020).

Games consist of multiple players, each with parameters and objectives. A solution is often defined to be a setting where no player gains from changing their strategy unilaterally, e.g., Nash equilibria (Morgenstern & Von Neumann, 1953) or Stackelberg equilibria (Von Stackelberg, 2010). Classical gradient-based learning often fails to find these equilibria due to rotational dynamics (Berard et al., 2019). Also, stationary points of naïve methods may not be desired solutions (Adolphs et al., 2019; Mazumdar et al., 2019).

Numerous algorithms for finding saddle points in zero-sum games have been proposed (Arrow et al., 1958; Freund & Schapire, 1999). Gidel et al. (2019) generalize GD with momentum to games, showing we can use a negative momentum to converge if the eigenvalues of the Jacobian of the learning dynamics have a large imaginary component. We use terminology in Gidel et al. (2019) and say (*purely/partially*) *adversarial or cooperative games* for games with (*purely/partially*) imaginary or real eigenvalues.

In this paper, we generalize negative momentum to complex momentum. Crucially, our parameter updates are real-valued, so our optimizer works on standard real-valued models, avoiding the difficulties of complex parameters (Dramsch et al., 2021; Trabelsi et al., 2017; Hirose, 2012).

Intuitively, our momentum buffer stores historical gradient information, oscillating between adding or subtracting it at a frequency dictated by our new hyperparameter – the phase of the momentum coefficient. This reduces rotational dynamics in parameter space by canceling out opposing updates. Classical and negative momentum are special cases of our approach, having phases of 0 and  $\pi$ . Classical momentum cannot handle oscillations due to rotations, and negative momentum corrects for oscillations at a specific (fixed) frequency. We correct for oscillations at an arbitrary (fixed) frequency and converge with simultaneous updates – a situation where negative momentum is known to fail.

## Contributions

- We propose a generalization of momentum for learning in differentiable games, which generalizes classical (Polyak, 1964; Nesterov, 1983; Sutskever et al., 2013) and negative momentum (Gidel et al., 2019).
- We show results describing the convergence rate of our method and prove we can converge on bilinear zero-sum games with simultaneous or alternating updates.
- We show a practical generalization of our method to a complex-valued Adam (Kingma & Ba, 2014) variant, which we use to train a BigGAN (Brock et al., 2018) on CIFAR-10, improving Inception scores.
- We combine our theory and empirical results to motivate a default setting for our new hyperparameter in partially adversarial games like GANs.

<sup>1</sup>University of Toronto <sup>2</sup>Vector Institute <sup>3</sup>NVIDIA. Correspondence to: <{lorraine, davidj, pvcicol, duvenaud}@cs.toronto.edu>.

## 2. Background

Table 2 in the Appendix summarizes our notation. Consider the optimization problem:

$$\theta^* := \arg \min_{\theta} \mathcal{L}(\theta) \quad (1)$$

We can find local minima of loss  $\mathcal{L}$  using (stochastic) gradient descent with step size  $\alpha$ . We denote the gradient of the loss at parameters  $\theta^j$  by  $g^j := g(\theta^j) := \nabla_{\theta} \mathcal{L}(\theta)|_{\theta^j}$ .

$$\theta^{j+1} = \theta^j - \alpha g^j \quad (\text{SGD})$$

Momentum can generalize **SGD**. For example, Polyak’s Heavy Ball (Polyak, 1964):

$$\theta^{j+1} = \theta^j - \alpha g^j + \beta(\theta^j - \theta^{j-1}) \quad (2)$$

Which can be equivalently written with momentum buffer  $\mu^j = (\theta^j - \theta^{j-1})/\alpha$ .

$$\mu^{j+1} = \beta \mu^j - g^j, \quad \theta^{j+1} = \theta^j + \alpha \mu^{j+1} \quad (\text{SGDm})$$

### 2.1. Game Formulations

Another class of problems is learning in *games*, which includes problems like generative adversarial networks (GANs) (Goodfellow et al., 2014). We focus on 2-player games —with players denoted by  $A$  and  $B$ —where each player minimizes their loss  $\mathcal{L}_A, \mathcal{L}_B$  with their parameters  $\theta_A \in \mathbb{R}^{d_A}, \theta_B \in \mathbb{R}^{d_B}$ . Solutions to 2-player games – which are assumed unique for simplicity – can be defined as:

$$\theta_A^* := \arg \min_{\theta_A} \mathcal{L}_A(\theta_A, \theta_B^*), \quad \theta_B^* := \arg \min_{\theta_B} \mathcal{L}_B(\theta_A^*, \theta_B) \quad (3)$$

In deep learning, losses are non-convex with many parameters, so we typically focus on finding local optima or local equilibria. Having an ordering to players, results in the special case of Stackelberg games. For example, in GANs, the generator is the leader, and the discriminator is the follower. In hyperparameter optimization, the hyperparameters are the leader, and the network parameters are the follower. If  $\theta_B^*(\theta_A)$  denotes player  $B$ ’s best-response function, then solutions to Stackelberg games can be defined as:

$$\begin{aligned} \theta_A^* &:= \arg \min_{\theta_A} \mathcal{L}_A(\theta_A, \theta_B^*(\theta_A)), \\ \theta_B^*(\theta_A) &:= \arg \min_{\theta_B} \mathcal{L}_B(\theta_A, \theta_B) \end{aligned} \quad (4)$$

If  $\mathcal{L}_A$  and  $\mathcal{L}_B$  are differentiable in  $\theta_A$  and  $\theta_B$  we say the game is differentiable. We may be able to approximately find  $\theta_A^*$  efficiently if we can do **SGD** on:

$$\mathcal{L}_A^*(\theta_A) := \mathcal{L}_A(\theta_A, \theta_B^*(\theta_A)) \quad (5)$$

Unfortunately, **SGD** would require computing  $\frac{d\mathcal{L}_A^*}{d\theta_A}$ , which often requires  $\frac{d\theta_B^*}{d\theta_A}$ , but  $\theta_B^*(\theta_A)$  and its Jacobian are typically intractable. A common optimization algorithm to

analyze for finding solutions is simultaneous **SGD** (**SSGD**) – sometimes called gradient descent ascent for zero-sum games – where  $g_A^j := g_A(\theta_A^j, \theta_B^j)$  and  $g_B^j := g_B(\theta_A^j, \theta_B^j)$  are estimators for  $\nabla_{\theta_A} \mathcal{L}_A|_{\theta_A^j, \theta_B^j}$  and  $\nabla_{\theta_B} \mathcal{L}_B|_{\theta_A^j, \theta_B^j}$ :

$$\theta_A^{j+1} = \theta_A^j - \alpha g_A^j, \quad \theta_B^{j+1} = \theta_B^j + \alpha g_B^j \quad (\text{SSGD})$$

We simplify notation by defining the joint parameters  $\omega := [\theta_A, \theta_B] \in \mathbb{R}^d$  and the game dynamics:

$$\hat{g}^j := \hat{g}(\omega^j) := [g_A(\omega^j), g_B(\omega^j)] = [g_A^j, g_B^j] \quad (6)$$

Our work extends to  $n$ -player games by treating  $\omega$  and  $\hat{g}$  as concatenations of the players’ parameters and loss gradients. This notation allows for a concise expression of the **SSGD** update with momentum (**SSGDm**):

$$\mu^{j+1} = \beta \mu^j - \hat{g}^j, \quad \omega^{j+1} = \omega^j + \alpha \mu^{j+1} \quad (\text{SSGDm})$$

Gidel et al. (2019) show the standard momentum choices of  $\beta \in [0, 1)$  do not improve solution speed over (**SSGD**) in some games, and that negative momentum can help when the Jacobian of the simultaneous game dynamics  $\nabla_{\omega} \hat{g}$  has complex eigenvalues. For bilinear zero-sum games, any non-negative momentum and step size will not converge, because the eigenvalues of  $\nabla_{\omega} \hat{g}$  are imaginary. For single-player games – i.e., minimization –  $\nabla_{\omega} \hat{g}$  has strictly real eigenvalues because it is the Hessian of our loss, which is often symmetric.

Motivated by obtaining convergence with simultaneous and alternating updates, we investigate solutions where optimizer parameters are complex. We want to guarantee the update to  $\omega$  is real-valued, so our parameters stay real-valued, and our optimizer can be a black-box, drop-in replacement for standard choices like **SGD** in deep learning pipelines.

## 3. Complex Momentum

Here, we describe our proposed method. We assume our momentum coefficient  $\beta \in \mathbb{C}$ , step size  $\alpha \in \mathbb{R}$ , momentum buffer  $\mu \in \mathbb{C}^d$ , and player parameters  $\omega \in \mathbb{R}^d$ . Derivations in the Appendix are done for  $\alpha \in \mathbb{C}$ , but in practice we only use real  $\alpha$ . The simultaneous (or Jacobi) update is:

$$\mu^{j+1} = \beta \mu^j - \hat{g}^j, \quad \omega^{j+1} = \omega^j + \Re(\alpha \mu^{j+1}) \quad (\text{Simul})$$

(**Simul**) is the standard choice in some settings, e.g., domain adversarial learning (Acuna et al., 2021). There are many ways to get a real-valued update from  $\mu \in \mathbb{C}$ , but we only consider updates equivalent to classical momentum when  $\beta \in \mathbb{R}$ . Specifically, we simply update the parameters using the real component of the momentum:  $\Re(\mu)$ .

We write the (**Simul**) update in Algorithm 1 and visualize it in Appendix Figure 10. We also show the alternating (or Gauss-Seidel) update, which is standard for GAN training:

$$\begin{aligned} \mu_A^{j+1} &= \beta \mu_A^j - \hat{g}_A(\omega^j), \quad \theta_A^{j+1} = \theta_A^j + \Re(\alpha \mu_A^{j+1}) \quad (\text{Alt}) \\ \mu_B^{j+1} &= \beta \mu_B^j - \hat{g}_B(\theta_A^{j+1}, \theta_B^j), \quad \theta_B^{j+1} = \theta_B^j + \Re(\alpha \mu_B^{j+1}) \end{aligned}$$

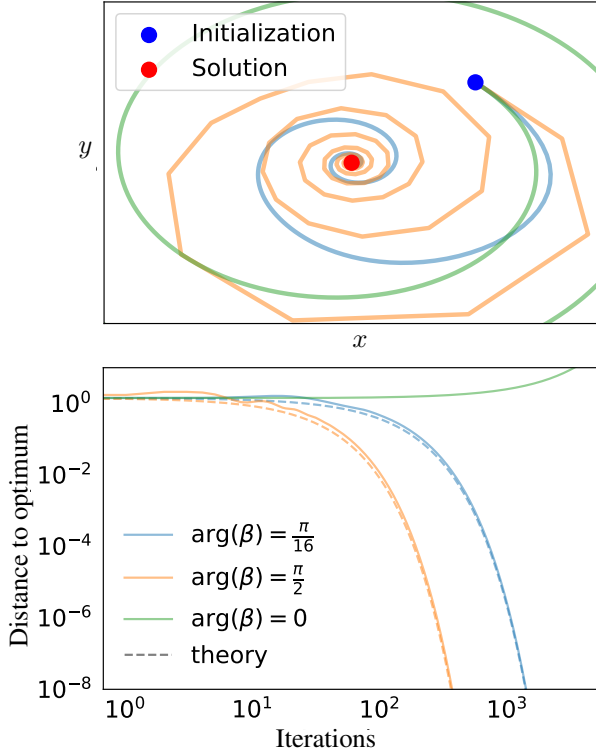


Figure 1: Complex momentum helps correct for rotational dynamics, with different momentum phases shown. *Top*: Trajectories on  $\min_x \max_y xy$  for the optimization parameters for the convergence proofs in Appendix A.3. We include the classical real, positive momentum  $\arg(\beta) = 0$  which diverges for any step size. *Bottom*: The distance from optimum, which has a linear convergence rate asymptotically matching our theories prediction.

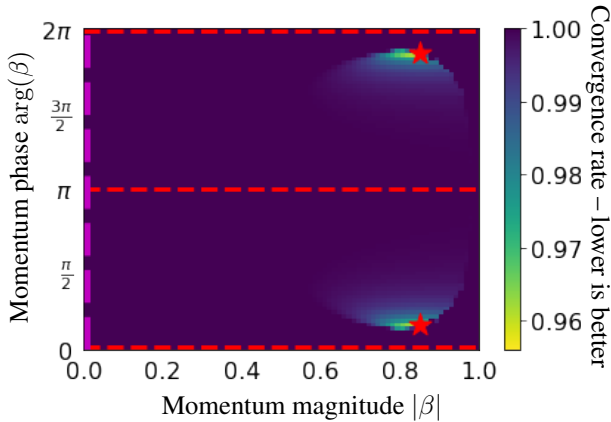


Figure 2: Convergence rates for simultaneous complex momentum on  $\min_x \max_y xy$ . The step size is fixed at  $\alpha = 0.1$ , while we vary the phase and magnitude of the complex momentum  $\beta = |\beta| \exp(i \arg(\beta))$ . There is a red star at the optima, dashed red lines at real  $\beta$ , and a dashed magenta line for simultaneous gradient descent. There are no real-valued  $\beta$  that converge for this – or any –  $\alpha$  with simultaneous updates (Gidel et al., 2019).

### Algorithm 1 (Simul) Momentum

```

1:  $\beta, \alpha \in \mathbb{C}, \mu \in \mathbb{C}^d, \omega^0 \in \mathbb{R}^d$ 
2: for  $i = 1 \dots N$  do
3:    $\mu^{j+1} = \beta \mu^j - \hat{g}^j$ 
4:    $\omega^{j+1} = \omega^j + \Re(\alpha \mu^{j+1})$ 
return  $\omega^N$ 
    
```

Consider the negative momentum from Gidel et al. (2019):

$$\omega^{j+1} = \omega^j - \alpha \hat{g}^j + \beta(\omega^j - \omega^{j-1}) \quad (7)$$

Expanding (Simul) with  $\mu^j = (\omega^j - \omega^{j-1})/\alpha$  for real momentum shows the negative momentum method of Gidel et al. (2019) is a special case of our method:

$$\omega^{j+1} = \omega^j + \Re(\alpha(\beta(\omega^j - \omega^{j-1})/\alpha - \hat{g}^j)) \quad (8)$$

$$= \omega^j - \alpha \hat{g}^j + \beta(\omega^j - \omega^{j-1}) \quad (9)$$

### 3.1. Dynamics of Complex Momentum

We provide proofs in the Appendix for the listed results. For simplicity, we assume Numpy-style (Harris et al., 2020) component-wise broadcasting for operations like modulus  $|z|$  or adding a scalar to a vector for  $z = [z_1, \dots, z_n] \in \mathbb{C}^n$ . Expanding the parameter updates with  $\alpha$  and  $\beta$  in terms of their Cartesian components is key for Theorem 1, which characterizes the convergence rate:

$$\begin{aligned} \mu^{j+1} &= \beta \mu^j - \hat{g}^j \iff \\ \Re(\mu^{j+1}) &= \Re(\beta) \Re(\mu^j) - \Im(\beta) \Im(\mu^j) - \Re(\hat{g}^j), \\ \Im(\mu^{j+1}) &= \Im(\beta) \Re(\mu^j) + \Re(\beta) \Im(\mu^j) \end{aligned} \quad (10)$$

$$\begin{aligned} \omega^{j+1} &= \omega^j + \Re(\alpha \mu^{j+1}) \iff \\ \omega^{j+1} &= \omega^j - \alpha \hat{g}^j + \Re(\alpha \beta) \Re(\mu^j) - \Im(\alpha \beta) \Im(\mu^j) \end{aligned} \quad (11)$$

(10) and (11) allow us to define our augmented dynamics of buffer  $\mu$  and parameters  $\omega$  when  $\mathcal{L}_{\{A/B\}}(\theta_A, \theta_B) = \theta_A^\top M_{\{A/B\}} \theta_A$ , because  $\Re(\hat{g}^j) = \nabla_{\omega} \hat{g} \cdot \omega^j$ :

$$\mathbf{R} := \begin{bmatrix} \Re(\beta) \mathbf{I} & -\Im(\beta) \mathbf{I} & -\nabla_{\omega} \hat{g} \\ \Im(\beta) \mathbf{I} & \Re(\beta) \mathbf{I} & 0 \\ \Re(\alpha \beta) \mathbf{I} & -\Im(\alpha \beta) \mathbf{I} & \mathbf{I} - \alpha \nabla_{\omega} \hat{g} \end{bmatrix} \quad (12)$$

So, our parameters evolve via:

$$[\Re(\mu^{j+1}), \Im(\mu^{j+1}), \omega^{j+1}]^\top = \mathbf{R} [\Re(\mu^j), \Im(\mu^j), \omega^j]^\top \quad (13)$$

We can bound the convergence rate with Theorem 1, which is a direct application of (13) with a well-known method for analyzing iterative methods (Polyak, 1964).

**Theorem 1** (Simultaneous Complex Momentum Convergence Rate). *Algorithm 1 with parameters  $\alpha, \beta \in \mathbb{C}$  for games of the form:*

$$\mathcal{L}_A(\theta_A, \theta_B) = \theta_A^\top M_A \theta_B, \mathcal{L}_B(\theta_A, \theta_B) = \theta_A^\top M_B \theta_B \quad (14)$$

*converges linearly with a rate  $\mathcal{O}(\rho(\mathbf{R}) + \epsilon)$ , if the spectral radius  $\rho(\mathbf{R}) < 1$ .*

Here, linear convergence means  $\lim_{j \rightarrow \infty} \frac{\|\omega^{j+1} - \omega^*\|}{\|\omega^j - \omega^*\|} \in (0, 1)$ , where  $\omega^*$  is a fixed point. We may want to express the spectrum of our augmented dynamics  $\text{Sp}(\mathbf{R}(\alpha, \beta))$ —with the dependence on  $\alpha$  and  $\beta$  now explicit—in terms of the spectrum  $\text{Sp}(\nabla_{\omega} \hat{g})$ , as in Theorem 3 in Gidel et al. (2019):

$$\mathbf{f}: \mathbb{C}^{d+2} \rightarrow \mathbb{C}^{3d}, \mathbf{f}(\text{Sp}(\nabla_{\omega} \hat{g}), \alpha, \beta) = \text{Sp}(\mathbf{R}(\alpha, \beta)) \quad (15)$$

We provide a Mathematica command in Appendix A.2 for a cubic polynomial  $p$  characterizing  $\mathbf{f}$  with coefficients that are functions of  $\alpha, \beta$  &  $\lambda \in \text{Sp}(\nabla_{\omega} \hat{g})$ , whose roots are eigenvalues of  $\mathbf{R}$ , which we use for the following results:

**Corollary 1** (Convergence of Complex Momentum). *There exist  $\alpha \in \mathbb{R}, \beta \in \mathbb{C}$  so Algorithm 1 converges for bilinear zero-sum games.*

This contrasts with a result of Gidel et al. (2019) who show that for all real  $\alpha, \beta$  Algorithm 1 *does not* converge. Empirically, in Section 4.2 at every non-real  $\beta = |\beta| \exp(i \arg(\beta))$  – i.e.,  $\arg(\beta) \neq 0$  or  $\pi$  – we could select  $\alpha, |\beta|$  so Algorithm 1 converges. We formalize this observation, by defining *almost-negative* or *almost-positive* to mean  $\arg(\beta) = \pi - \epsilon$  or  $\arg(\beta) = \epsilon$  for small  $\epsilon$  respectively, and showing there are complex  $\beta$  which are almost-negative or positive that converge.

**Corollary 2** (Almost-real Momentum can Converge). *For small  $\epsilon$  (we show for  $\epsilon = \frac{\pi}{16}$ ), if  $\arg(\beta) = \pi - \epsilon$  (i.e., almost-negative) or  $\arg(\beta) = \epsilon$  (i.e., almost-positive), then we can select  $\alpha, |\beta|$  so Algorithm 1 converges on bilinear zero-sum games.*

This result suggests we should use complex, almost-positive momentum, which may be beneficial in games with real and imaginary eigenvalues in  $\text{Sp}(\nabla_{\omega} \hat{g})$ , because positive  $\beta$  are optimal in the real eigenspaces, and almost-positive  $\beta$  can work for imaginary eigenspaces. We conjecture that almost-positive  $\beta$  may work best on games with mixed real and imaginary eigenvalues like GANs – which is verified by experiments in Sections 4.2, 4.3, and 4.4.

Which  $\alpha$  and  $\beta$  have the best convergence rate? We show the term being expanded in red to show how Theorem 1 and (15) can help find optimal  $\alpha^*, \beta^*$  and convergence rate  $\rho^*$ :

$$\alpha^*, \beta^* := \arg \min_{\alpha, \beta} \rho(\mathbf{R}(\alpha, \beta)) \quad (16)$$

$$= \arg \min_{\alpha, \beta} \max_{z \in \text{Sp}(\mathbf{R}(\alpha, \beta))} |z| = \arg \min_{\alpha, \beta} \max_{z \in \mathbf{f}(\text{Sp}(\nabla_{\omega} \hat{g}), \alpha, \beta)} |z| \quad (17)$$

$$\rho^* := \rho(\mathbf{R}(\alpha^*, \beta^*)) \quad (18)$$

We use  $\rho(\mathbf{R}(\alpha, \beta)) = \max_{z \in \mathbf{f}(\text{Sp}(\nabla_{\omega} \hat{g}), \alpha, \beta)} |z|$  in Section 4.2. We could not analytically solve for  $\alpha^*, \beta^*$ , so the arg min is approximated by a grid search in our experiments.

### 3.2. What about Acceleration?

With classical momentum, (16) and (18) are tractable if  $0 < l \leq L$  and  $\text{Sp}(\nabla_{\omega} \hat{g}) \in [l, L]^d$  (Goh, 2017) – i.e., we have an  $l$ -strongly convex and  $L$ -Lipschitz loss, where the conditioning  $\kappa = L/l$  can characterize problem difficulty. Gradient descent with an appropriate  $\alpha$  can achieve a convergence rate of  $\frac{\kappa-1}{\kappa+1}$ , but using momentum with appropriate  $(\alpha^*, \beta^*)$  can achieve an *accelerated* rate of  $\rho^* = \frac{\sqrt{\kappa-1}}{\sqrt{\kappa+1}}$ .

However, there is no consensus for constraining  $\text{Sp}(\nabla_{\omega} \hat{g})$  in games for tractable and useful results. Candidate constraints include monotonic vector fields generalizing notions of convexity, or vector fields with bounded eigenvalue norms capturing a kind of sensitivity (Azizian et al., 2020a).

Figure 9 shows  $\text{Sp}(\nabla_{\omega} \hat{g})$  for a GAN – we can attribute some eigenvectors to a single player’s parameters. The discriminator can be responsible for the largest and smallest norm eigenvalues, suggesting we vary  $\alpha$  and  $\beta$  for each player. Generalizing (16) and (18) to see if we can accelerate for a notion of conditioning is left to future work.

### 3.3. Implementing Complex Momentum

Complex momentum is trivial to implement with libraries supporting complex arithmetic like Jax (Bradbury et al., 2018) or Pytorch (Paszke et al., 2017). Given an SGD implementation, we often only need to change a few lines of code. Figure 8 has all changes necessary Jax’s SGD with momentum implementation, which amounts to changing a single line and giving it a complex momentum coefficient (or mass). Also, (10) and (11) can be easily used to implement Algorithm 1 in a library without complex arithmetic.

The computational cost is almost identical to **SGDm**, except we now have a buffer with twice as many real parameters. More sophisticated optimizers like Adam can trivially support complex optimizer parameters with real-valued updates, which we explore in Section 4.4.

## 4. Experiments

Our experiments investigate how complex momentum performs in adversarial games. We investigate the method by running it and analyzing the spectrum on bilinear games and GANs. Reproducibility details are in Appendix C. Code for the experiments will be made available on publication.

We start with bilinear zero-sum games, which are purely adversarial and have a known solution  $\omega^* = (\theta_A^*, \theta_B^*)$ . Next, we evaluate GANs generating 2-D distributions, because we can visualize them, assess performance with log-likelihood, and train with a plain, alternating SGD. Finally, we evaluate larger-scale GANs on images, where it is difficult to determine the solution quality, so we use proxy measures like Inception Score (IS) (Salimans et al., 2016).

#### 4.1. Optimization in Bilinear Zero-Sum Games

Here, we consider the same bilinear game as Gidel et al. (2019), which is surprisingly hard and where many classical optimization methods fail, because  $\text{Sp}(\nabla_{\omega} \hat{g})$  is imaginary:

$$\min_x \max_y xy \quad (19)$$

See Zhang & Yu (2019) for further analysis of bilinear problems. Figure 1 shows the optimization trajectories of simultaneous updates, empirically verifying convergence rates given by Theorem 1 and the proofs of Corollary 1 & 2.

Next, we fix  $\alpha$  and vary both  $|\beta|$  and  $\arg(\beta)$ . We plot  $\alpha = 0.1$  to observe behavior with small step sizes. Figure 2 shows a heatmap of these results with simultaneous updates, where  $\beta$  must be complex to converge. Here, the best  $\beta$  was almost-positive (i.e.,  $\arg(\beta) = \epsilon$  for small  $\epsilon$ ). We repeat the heatmap with alternating updates and the same  $\alpha$  in Appendix Figure 11, where almost-positive momentum still converges fastest, but negative momentum also converges.

#### 4.2. Spectrum of the Augmented Dynamics

Here, we investigate the spectrum of the augmented dynamics  $\text{Sp}(\mathbf{R})$  for games of the form:

$$\min_x \max_y \gamma \mathbf{x}^\top \mathbf{A} \mathbf{y} + (1 - \gamma)(\mathbf{x}^\top \mathbf{B}_1 \mathbf{x} - \mathbf{y}^\top \mathbf{B}_2 \mathbf{y}) \quad (20)$$

If  $\gamma = 1$  the game is purely adversarial, while if the  $\gamma = 0$  the game is purely cooperative.

Figure 3 shows  $\text{Sp}(\mathbf{R})$  on purely adversarial games for a range of  $\alpha$  and  $\beta$ , generalizing Figure 4 in Gidel et al. (2019). For every non-real  $\beta$ —i.e.,  $\arg(\beta) \neq \pi$  or  $0$ —we could select  $\alpha$  and  $|\beta|$  that converge.

Figure 4 compares different  $\arg(\beta)$  on games by interpolating from purely cooperative to purely adversarial by taking  $\gamma$  from 1 to 0. At each  $\arg(\beta)$  we do a grid search to tune  $|\beta|, \alpha$ . The optimal  $\arg(\beta)$  depends on how adversarial the game is. When the game is (almost) cooperative the best  $\beta$  are (almost) positive. But, as the game becomes more adversarial, more imaginary  $\beta$  perform better. Negative momentum does not work best for any game.

Complex momentum may work better than negative momentum for games that are not purely adversarial, because it can work with almost-positive momentum  $\beta$ . Figure 9 shows a GAN with many real eigenvalues during training, displaying that GANs are not purely adversarial.

#### 4.3. Training GANs on 2-Dimensional Distributions

In these experiments, we train GANs to generate a 2-D mixture of Gaussians using alternating SGD updates with complex momentum. Figure 8 shows all changes necessary to use the Jax momentum optimizer for our updates, with full experimental details in Appendix C.4.

We evaluate the log-likelihood of GAN samples under the mixture as an imperfect proxy for matching. Figure 5 shows heatmaps for tuning  $\arg(\beta)$  and  $|\beta|$  with fixed step sizes. The best  $\arg(\beta)$  was found at the almost-positive value of  $\beta \approx 0.7 \exp(i\pi/8)$ , whose samples are shown in Figure 7.

#### 4.4. Training BigGAN with a Complex Adam

We trained BigGAN with complex momentum (Brock et al., 2018) on CIFAR-10 (Krizhevsky, 2009). GANs are notoriously brittle during optimization, so we change the procedure minimally. We took the author-supplied code at <https://github.com/ajbrock/BigGAN-PyTorch>, which was trained with Adam, and made the  $\beta_1$  parameter – which is analogous to momentum – complex.

The modified complex Adam is shown in Algorithm 2, where we removed the momentum bias correction to better match our theory. It remains an open question on how to best carry over the original design of Adam (or other optimizers) to the complex setting.

Figure 6 shows a grid search over  $\arg(\beta_1), |\beta_1|$  for BigGAN trained with Algorithm 2. We kept the optimizer parameters for the generator the same and only changed  $\beta_1$  for the discriminator’s optimizer. The best momentum value was at the almost-positive value of  $\beta_1 \approx 0.8 \exp(i\pi/8)$ .

---

**Algorithm 2** Complex Adam variant without momentum bias-correction

---

```

1:  $\beta_1 \in \mathbb{C}, \beta_2 \in [0, 1], \alpha \in \mathbb{R}^+, \epsilon \in \mathbb{R}^+$ 
2: for  $j = 1 \dots N$  do
3:    $\mu^j = \beta_1 \mu - \mathbf{g}^j$ 
4:    $\mathbf{v}^j = \beta_2 \mathbf{v} + (1 - \beta_2)(\mathbf{g} * *2)$ 
5:    $\hat{\mathbf{v}}^j = \frac{\mathbf{v}^j}{1 - \beta_2^{**j}}$ 
6:    $\omega^{j+1} = \omega^j + \alpha \frac{\Re(\mu^j)}{\sqrt{\hat{\mathbf{v}}^j + \epsilon}}$ 
return  $\omega^N$ 
    
```

---

We tested the best momentum value over 10 seeds against the author-provided baseline in Appendix Figure 13, with the results summarized in Table 1. The BigGAN authors reported a single inception score (IS) on CIFAR-10 of 9.22, but the best we could reproduce over the seeds with the provided PyTorch code and settings was 9.1. Our momentum coefficient improves the best IS found over the runs with 9.25(+.15 author code, +.03 author reported).

We tried training a real momentum with a magnitude of 0.8 to see if the improvement was solely due to tuning  $|\beta_1|$ . This occasionally failed to train and decreased the best IS over re-runs, showing we benefit from a non-zero  $\arg(\beta_1)$ .

Training each BigGAN took 10 hours on an NVIDIA T4 GPU, so Figure 6 and Table 1 took about 1000 and 600 GPU hours respectively.

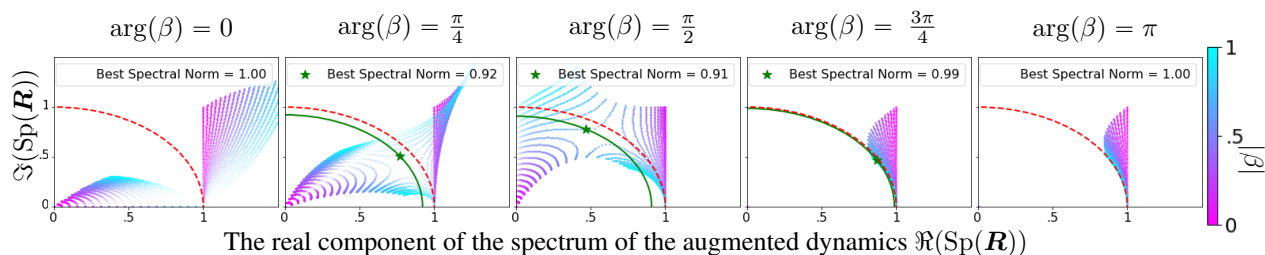


Figure 3: The spectrum of the augmented dynamics  $\mathbf{R}$  is shown, whose spectral norm is the convergence rate in Theorem 1. Each image is a different momentum phase  $\arg(\beta)$  for a range of  $\alpha, |\beta| \in [0, 1]$ . The opacity of an eigenvalue (eig) is the step size  $\alpha$  and the color corresponds to momentum magnitude  $|\beta|$ . A red unit circle shows where all eigs must lie to converge for a fixed  $\alpha, \beta$ . If the max eig norm  $< 1$ , we draw a green circle whose radius is our convergence rate and a green star at the associated eig. Notably, at every non-real  $\beta$  we can select  $\alpha, |\beta|$  for convergence. The eigs are symmetric over the  $x$ -axis, and eigs near  $\Re(\lambda) = 1$  dictate convergence rate. Eigs near the center are due to state augmentation, have small magnitudes, and do not impact convergence rate. Simultaneous gradient descent corresponds to the magenta values where  $|\beta| = 0$ .

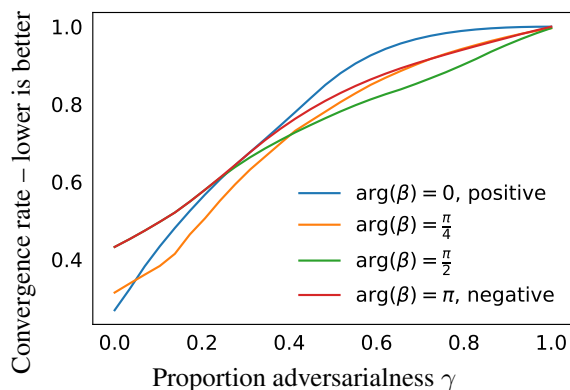


Figure 4: We compare optimal convergence rates for various  $\arg(\beta)$  on a range of games defined in (20), where  $\mathbf{A}$  and  $\mathbf{B}$  are diagonal with entries in  $[1/2, 2]$ . We interpolate from purely cooperative to purely adversarial. At each  $\arg(\beta)$  we do a grid search to find the best  $|\beta|, \alpha$ . In cooperative games a positive momentum (i.e.,  $\arg(\beta) = 0$ ) is best, but partially adversarial games can benefit from non-zero  $\arg(\beta)$ . Negative momentum (i.e.,  $\arg(\beta) = \pi$ ) never performs best.

CIFAR-10 BigGAN Discriminator $\beta_1$	Best IS for 10 seeds	
	Min	Max
0 – author default	8.9	9.1
$0.8 \exp(i\pi/8)$	8.96(+.06)	9.25(+.15)
0.8	3.12(-5.78)	9.05(-0.05)

Table 1: We display the best inception scores (IS) found over 10 runs for training BigGAN on CIFAR-10 with various optimizer settings. We use a complex Adam variant outlined in Algorithm 2, where we only tuned  $\beta_1$  for the discriminator. The best parameters found in Figure 6 were  $\beta_1 = 0.8 \exp(i\pi/8)$ , which improved the min and max IS from our runs of the BigGAN authors baseline. We tested  $\beta_1 = 0.8$  to see if the gain was solely from tuning  $|\beta_1|$ , which occasionally failed and decreased the best IS.

#### 4.5. Default Optimizer Parameters

Motivated by our empirical and theoretical results we propose a default setting for our new hyperparameter. Corollary 2 shows that we can use almost-real momentum coefficients (i.e.,  $\arg(\beta)$  is close to  $\pi$  or 0). Figure 4 shows that we may want almost-positive  $\beta$  for partially adversarial games. Figure 9 shows that some GANs have both real and imaginary eigenvalues at the end of training, so they are partially adversarial. Figures 5 and 6 do a grid search over  $\arg(\beta)$  and  $|\beta|$  for 2-D and image GANs, finding that almost-positive  $\arg(\beta) \approx \pi/8$  works in both cases.

Based on this evidence, we propose a default value of  $\arg(\beta) = \pi/8$  for GANs. This arg may be by a small enough perturbation, that we can minimally change the other hyperparameters in our model. This is useful to adapt existing, brittle setups like in GAN optimization.

## 5. Related Work

**Accelerated First-order Methods:** There is a broad body of work leveraging momentum-type methods (Polyak, 1964; Nesterov, 1983; 2013; Maddison et al., 2018), with a recent focus on deep learning (Sutskever et al., 2013; Zhang & Mitliagkas, 2017; Choi et al., 2019; Zhang et al., 2019; Chen et al., 2020). But, these works focus on momentum for minimization as opposed to momentum in game dynamics. Lucas et al. (2018) propose multiple momentum buffers, like our real and imaginary components. However, we look at games and recurrently link the buffers.

**Learning in Games:** Various works approximate response-gradients - some by differentiating through optimization (Foster et al., 2018; Mescheder et al., 2017; Maclaurin et al., 2015). Sometimes response gradients can be unstable, motivating methods like Stable Opponent Shaping (Letcher et al., 2019). Various works use higher-order information to help games, or approximate a large matrix inversion (Hemmat et al., 2020; Wang et al., 2019; Schäfer & Anandkumar,

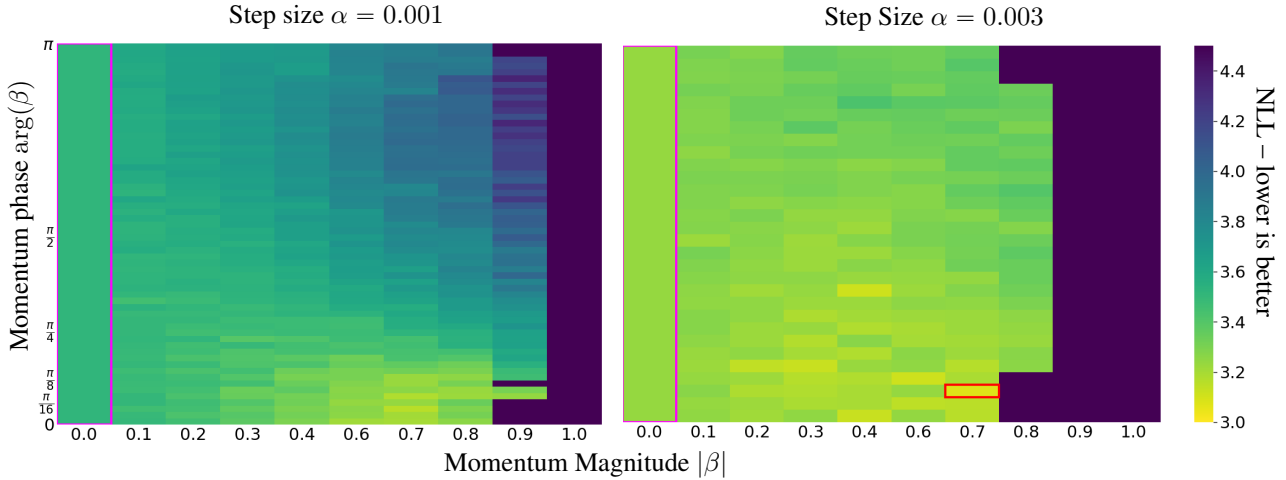


Figure 5: Heatmaps of the negative log-likelihood (NLL) for tuning  $\arg(\beta)$ ,  $|\beta|$  with various fixed  $\alpha$  on a 2-D mixture of Gaussians GAN. We highlight the best performing cell in red, which had  $\arg(\beta) \approx \pi/8$ . Runs equivalent to alternating SGD are shown in a magenta box. We compare to negative momentum with alternating updates as in Gidel et al. (2019) in the top row with  $\arg(\beta) = \pi$ . Left: Tuning the momentum with  $\alpha = 0.001$ . Right: Tuning the momentum with  $\alpha = 0.003$ .

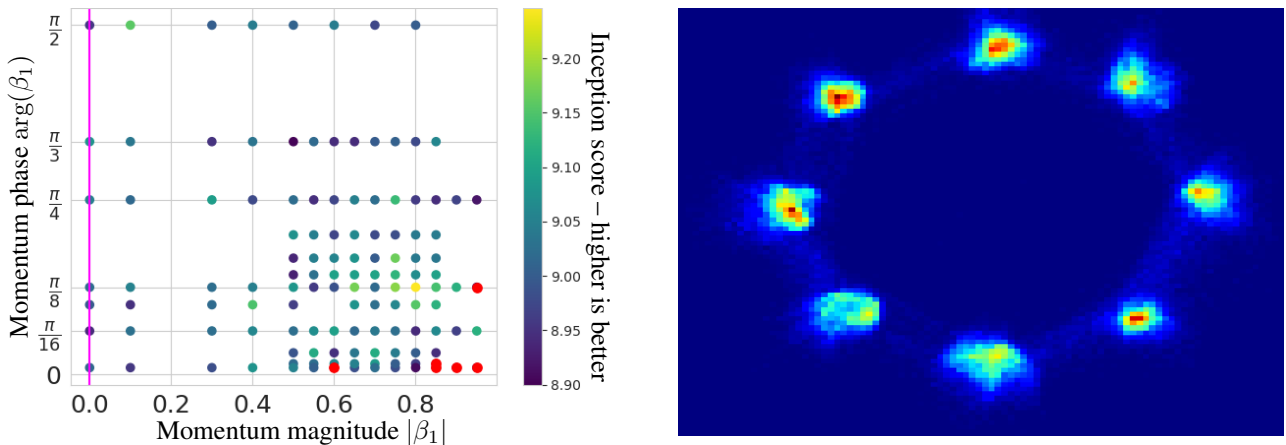


Figure 6: The inception score (IS) for a grid search on  $\arg(\beta_1)$  and  $|\beta_1|$  for training BigGAN on CIFAR-10 with the Adam variant in Algorithm 2. The  $\beta_1$  is complex for the discriminator, while the generator’s optimizer is fixed to author-supplied defaults. Red points are runs that failed to train to the minimum IS in the color bar. The vertical magenta line denotes runs equivalent to alternating SGD.

2019; Schäfer et al., 2020; Czarnecki et al., 2020), which can be difficult to scale, and it can be unclear is lost by approximations. We can decompose into a Hamiltonian and potential game (Letcher et al., 2019). Multiple works look at structure in games (Nagarajan et al., 2020; Omidshafiei et al., 2020; Czarnecki et al., 2020; Gidel et al., 2020; Perolat et al., 2020).

**First-order Methods in Games:** For some games, we need higher than first-order information for a method that con-

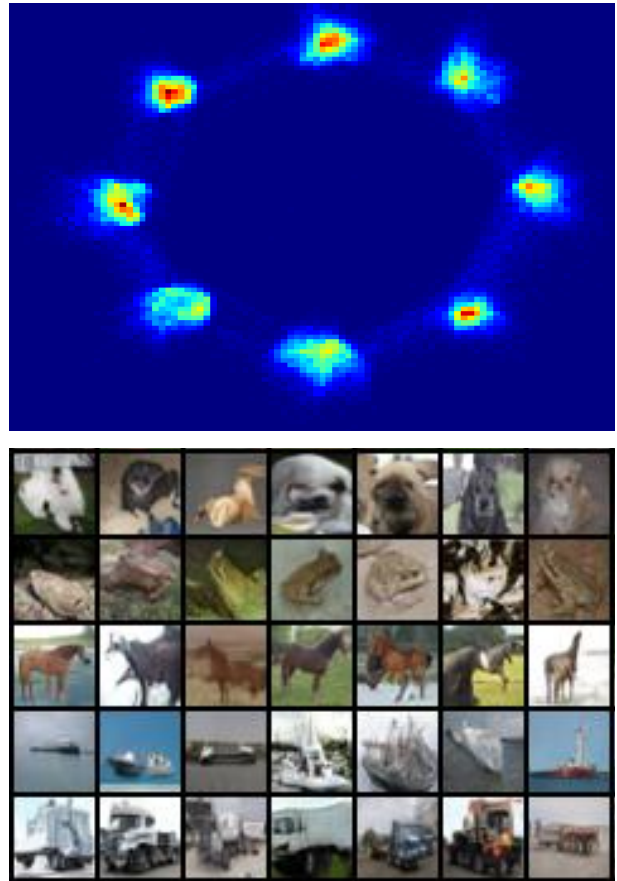


Figure 7: Samples from GANs with the best hyperparameters for heatmaps in Figures 5 and 6. Top: Mixture of Gaussians. Bottom: Class-conditional CIFAR-10.

verges. An example is pure-response games (Lorrain et al., 2020) because the first-order information for a player is identically zero. However, in some games, we can get away with using only first-order methods like extragradient (Korpelevich, 1976; Jelassi et al., 2020). Zhang et al. (2020); Ibrahim et al. (2020); Bailey et al. (2020); Jin et al. (2020); Azizian et al. (2020a); Nouiehed et al. (2019) discuss when and how some first-order methods will work on games. Gidel et al. (2019) is the closest work to ours, showing a negative momentum can help in some games. Zhang & Yu (2019) note the suboptimality of negative momentum in a class of games. Azizian et al. (2020b); Domingo-Enrich et al. (2020) investigate acceleration in some games.

**Bilinear Games:** Zhang & Yu (2019) study the convergence of gradient methods in bilinear zero-sum games. Their analysis extends Gidel et al. (2019), showing that we can achieve faster convergence by having separate step sizes and momentum for each player or tuning the extragradient step size. Loizou et al. (2020) provide convergence guarantees for games satisfying a *sufficiently bilinear* condition.

**Learning in GANs:** Various works try to make GAN training easier with methods leveraging the game structure (Liu et al., 2020; Peng et al., 2020; Albuquerque et al., 2019; Wu et al., 2019; Hsieh et al., 2019). Metz et al. (2016) approximate the discriminator’s response function by differentiating through optimization. Mescheder et al. (2017) find solutions by minimizing the norm of the players’ updates. Both of these methods and various others (Qin et al., 2020; Schäfer et al., 2019; Jolicoeur-Martineau & Mitliagkas, 2019) require higher-order information – Hessian-vector products – which are efficient with automatic differentiation tools like PyTorch. Daskalakis et al. (2018) approximate the extragradient update with a prior gradient, while Gidel et al. (2018); Chavdarova et al. (2019) use extragradient updates or averaging. Mescheder et al. (2018) explore problems for GAN training convergence and Berard et al. (2019) show that GANs have significant rotations affecting learning.

## 6. Conclusion

In this paper, we generalized gradient descent with momentum for learning in differentiable games, by allowing complex-valued momentum with real-valued updates. We gave theoretical motivation for our method on bilinear zero-sum games. We empirically showed that complex-valued momentum can improve convergence in partially adversarial games like GANs. We presented a complex Adam variant which we used to train BigGAN. Finally, we combined our theoretical and empirical results to propose a potential default value for our new optimization hyperparameter – the phase of the momentum coefficient  $\arg(\beta)$ . We view this as a step towards generalizing popular optimizers to large-scale, partially adversarial games.

```

Actual Jax implementation of complex momentum
@optimizer
def momentum(step_size, mass):
    ...
    def update(i, g, state):
        x, velocity = state
        velocity = mass * velocity + g
        x = x - jnp.real(step_size(i)*velocity)
        return x, velocity
    ...

```

Figure 8: We show how to modify Jax’s SGD with momentum implementation here to use complex momentum. The only change is shown in red. `jnp.real` gets the real part of `step_size` times the momentum buffer (called `velocity` here). We can use a complex mass for our method, such as `mass = .7*jnp.exp(1j*(jnp.pi/8))` for a momentum  $\beta = |\beta| \exp(i \arg(\beta)) = 0.7 \exp(i\pi/8)$  as in experiments for Figure 5.

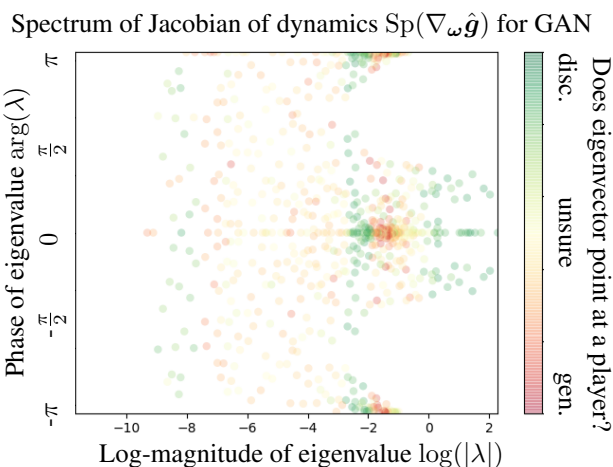


Figure 9: A log-polar coordinate visualization reveals structure in the spectrum for a GAN at the end of the training on a 2-D mixture of Gaussians with a 1-layer discriminator (disc.) and generator (gen.), so the concatenated parameters  $\omega \in \mathbb{R}^{723}$ . Appendix Figure 12 shows how the spectrum changes through training.

There are real (i.e.,  $\arg(\lambda) \approx 0, \pm\pi$ ) and imaginary (i.e.,  $\arg(\lambda) \approx \pm\frac{\pi}{2}$ ) eigenvalues, so – contrary to what the name may suggest – generative adversarial networks are not purely adversarial (or cooperative).

Eigenvalues are colored if the associated eigenvector lies mostly in a single player’s part of the concatenated parameter space – see Appendix Figure 12 for details on this. Many eigenvectors lie mostly in the the space of (or point at) a single player. The structure of the set of eigenvalues for the discriminator (green) is different than the generator (red), but further investigation of this is an open problem. This may motivate separate optimizer choices for each player. It is difficult to see structure by graphing the Cartesian (i.e.,  $\Re$  and  $\Im$ ) parts of eigenvalues, because they span orders of magnitude, while being positive and negative.



## Acknowledgements

Resources used in preparing this research were provided, in part, by the Province of Ontario, the Government of Canada through CIFAR, and companies sponsoring the Vector Institute. Paul Vicol was supported by an NSERC PGS-D Scholarship. We thank James Lucas, Romina Abachi, Jonah Phillion, Will Grathwohl, Jakob Foerster, Murat Erdogdu, Ken Jackson, and Ioannis Mitliagkis for feedback and helpful discussion.

## References

- Abachi, R., Ghavamzadeh, M., and Farahmand, A.-m. Policy-aware model learning for policy gradient methods. *arXiv preprint arXiv:2003.00030*, 2020. [Cited on page 1]
- Acuna, D., Zhang, G., Law, M. T., and Fidler, S. f-domain-adversarial learning: Theory and algorithms for unsupervised domain adaptation with neural networks, 2021. URL <https://openreview.net/forum?id=WqXAKcwfZtI>. [Cited on pages 1 and 2]
- Adam, G. and Lorraine, J. Understanding neural architecture search techniques. *arXiv preprint arXiv:1904.00438*, 2019. [Cited on page 1]
- Adolphs, L., Daneshmand, H., Lucchi, A., and Hofmann, T. Local saddle point optimization: A curvature exploitation approach. In *The 22nd International Conference on Artificial Intelligence and Statistics*, pp. 486–495. PMLR, 2019. [Cited on page 1]
- Albuquerque, I., Monteiro, J., Doan, T., Considine, B., Falk, T., and Mitliagkas, I. Multi-objective training of generative adversarial networks with multiple discriminators. In *International Conference on Machine Learning*, pp. 202–211. PMLR, 2019. [Cited on page 8]
- Arrow, K. J., Azawa, H., Hurwicz, L., and Uzawa, H. *Studies in Linear and Non-Linear Programming*, volume 2. Stanford University Press, 1958. [Cited on page 1]
- Azizian, W., Mitliagkas, I., Lacoste-Julien, S., and Gidel, G. A tight and unified analysis of gradient-based methods for a whole spectrum of differentiable games. In *International Conference on Artificial Intelligence and Statistics*, pp. 2863–2873. PMLR, 2020a. [Cited on pages 4 and 8]
- Azizian, W., Scieur, D., Mitliagkas, I., Lacoste-Julien, S., and Gidel, G. Accelerating smooth games by manipulating spectral shapes. *arXiv preprint arXiv:2001.00602*, 2020b. [Cited on page 8]
- Bacon, P.-L., Schäfer, F., Gehring, C., Anandkumar, A., and Brunskill, E. A Lagrangian method for inverse problems in reinforcement learning. *lis.csail.mit.edu/pubs*, 2019. [Cited on page 1]
- Bailey, J. P., Gidel, G., and Piliouras, G. Finite regret and cycles with fixed step-size via alternating gradient descent-ascent. In *Conference on Learning Theory*, pp. 391–407. PMLR, 2020. [Cited on page 8]
- Baker, B., Kanitscheider, I., Markov, T., Wu, Y., Powell, G., McGrew, B., and Mordatch, I. Emergent tool use from multi-agent autotutorials. In *International Conference on Learning Representations*, 2019. [Cited on page 1]
- Balduzzi, D., Garnelo, M., Bachrach, Y., Czarnecki, W., Perolat, J., Jaderberg, M., and Graepel, T. Open-ended learning in symmetric zero-sum games. In *International Conference on Machine Learning*, pp. 434–443. PMLR, 2019. [Cited on page 1]
- Berard, H., Gidel, G., Almahairi, A., Vincent, P., and Lacoste-Julien, S. A closer look at the optimization landscapes of generative adversarial networks. In *International Conference on Learning Representations*, 2019. [Cited on pages 1 and 8]
- Bertsekas, D. *Nonlinear Programming*. Athena Scientific, 2008. [Cited on page 15]
- Bose, A. J., Gidel, G., Berrard, H., Cianflone, A., Vincent, P., Lacoste-Julien, S., and Hamilton, W. L. Adversarial example games. *arXiv preprint arXiv:2007.00720*, 2020. [Cited on page 1]
- Bradbury, J., Frostig, R., Hawkins, P., Johnson, M. J., Leary, C., Maclaurin, D., and Wanderman-Milne, S. JAX: composable transformations of Python+NumPy programs, 2018. URL <http://github.com/google/jax>. [Cited on page 4]
- Brock, A., Donahue, J., and Simonyan, K. Large scale gan training for high fidelity natural image synthesis. In *International Conference on Learning Representations*, 2018. [Cited on pages 1 and 5]
- Chavdarova, T., Gidel, G., Fleuret, F., and Lacoste-Julien, S. Reducing noise in gan training with variance reduced extragradient. In *Proceedings of the international conference on Neural Information Processing Systems*, number CONF, 2019. [Cited on page 8]
- Chen, R. T., Choi, D., Balles, L., Duvenaud, D., and Hennig, P. Self-tuning stochastic optimization with curvature-aware gradient filtering. *arXiv preprint arXiv:2011.04803*, 2020. [Cited on page 6]
- Choi, D., Shallue, C. J., Nado, Z., Lee, J., Maddison, C. J., and Dahl, G. E. On empirical comparisons of optimizers for deep learning. *arXiv preprint arXiv:1910.05446*, 2019. [Cited on page 6]

- Czarnecki, W. M., Gidel, G., Tracey, B., Tuyls, K., Omidshafiei, S., Balduzzi, D., and Jaderberg, M. Real world games look like spinning tops. *arXiv preprint arXiv:2004.09468*, 2020. [Cited on page 7]
- Daskalakis, C., Ilyas, A., Syrgkanis, V., and Zeng, H. Training gans with optimism. In *International Conference on Learning Representations (ICLR 2018)*, 2018. [Cited on page 8]
- Domingo-Enrich, C., Pedregosa, F., and Scieur, D. Average-case acceleration for bilinear games and normal matrices. *arXiv preprint arXiv:2010.02076*, 2020. [Cited on page 8]
- Dramsach, J. S., Lüthje, M., and Christensen, A. N. Complex-valued neural networks for machine learning on non-stationary physical data. *Computers & Geosciences*, 146:104643, 2021. [Cited on page 1]
- Foerster, J., Chen, R. Y., Al-Shedivat, M., Whiteson, S., Abbeel, P., and Mordatch, I. Learning with opponent-learning awareness. In *International Conference on Autonomous Agents and MultiAgent Systems*, pp. 122–130, 2018. [Cited on page 6]
- Foucart, S. Matrix norm and spectral radius. <https://www.math.drexel.edu/~foucart/TeachingFiles/F12/M504Lect6.pdf>, 2012. Accessed: 2020-05-21. [Cited on page 16]
- Freund, Y. and Schapire, R. E. Adaptive game playing using multiplicative weights. *Games and Economic Behavior*, 29(1-2):79–103, 1999. [Cited on page 1]
- Gidel, G., Berard, H., Vignoud, G., Vincent, P., and Lacoste-Julien, S. A variational inequality perspective on generative adversarial networks. In *International Conference on Learning Representations*, 2018. [Cited on page 8]
- Gidel, G., Hemmat, R. A., Pezeshki, M., Le Priol, R., Huang, G., Lacoste-Julien, S., and Mitliagkas, I. Negative momentum for improved game dynamics. In *The 22nd International Conference on Artificial Intelligence and Statistics*, pp. 1802–1811. PMLR, 2019. [Cited on pages 1, 2, 3, 4, 5, 7, 8, 16, 17, and 19]
- Gidel, G., Balduzzi, D., Czarnecki, W. M., Garnelo, M., and Bachrach, Y. Minimax theorem for latent games or: How i learned to stop worrying about mixed-nash and love neural nets. *arXiv preprint arXiv:2002.05820*, 2020. [Cited on page 7]
- Goh, G. Why momentum really works. *Distill*, 2(4):e6, 2017. [Cited on page 4]
- Goodfellow, I., Pouget-Abadie, J., Mirza, M., Xu, B., Warde-Farley, D., Ozair, S., Courville, A., and Bengio, Y. Generative adversarial nets. In *Advances in Neural Information Processing Systems*, pp. 2672–2680, 2014. [Cited on pages 1, 2, and 13]
- Grathwohl, W., Creager, E., Ghasemipour, S. K. S., and Zemel, R. Gradient-based optimization of neural network architecture. 2018. [Cited on page 1]
- Hahnloser, R. H., Sarpeshkar, R., Mahowald, M. A., Douglas, R. J., and Seung, H. S. Digital selection and analogue amplification coexist in a cortex-inspired silicon circuit. *Nature*, 405(6789):947–951, 2000. [Cited on page 19]
- Harris, C. R., Millman, K. J., van der Walt, S. J., Gommers, R., Virtanen, P., Cournapeau, D., Wieser, E., Taylor, J., Berg, S., Smith, N. J., et al. Array programming with numpy. *Nature*, 585(7825):357–362, 2020. [Cited on page 3]
- Hemmat, R. A., Mitra, A., Lajoie, G., and Mitliagkas, I. Lead: Least-action dynamics for min-max optimization. *arXiv preprint arXiv:2010.13846*, 2020. [Cited on page 6]
- Hirose, A. *Complex-valued neural networks*, volume 400. Springer Science & Business Media, 2012. [Cited on page 1]
- Hsieh, Y.-P., Liu, C., and Cevher, V. Finding mixed nash equilibria of generative adversarial networks. In *International Conference on Machine Learning*, pp. 2810–2819. PMLR, 2019. [Cited on page 8]
- Ibrahim, A., Azizian, W., Gidel, G., and Mitliagkas, I. Linear lower bounds and conditioning of differentiable games. In *International Conference on Machine Learning*, pp. 4583–4593. PMLR, 2020. [Cited on page 8]
- Jelassi, S., Domingo-Enrich, C., Scieur, D., Mensch, A., and Bruna, J. Extra-gradient with player sampling for faster convergence in n-player games. In *International Conference on Machine Learning*, pp. 4736–4745. PMLR, 2020. [Cited on page 8]
- Jin, C., Netrapalli, P., and Jordan, M. What is local optimality in nonconvex-nonconcave minimax optimization? In *International Conference on Machine Learning*, pp. 4880–4889. PMLR, 2020. [Cited on page 8]
- Jolicoeur-Martineau, A. and Mitliagkas, I. Connections between support vector machines, wasserstein distance and gradient-penalty gans. *arXiv preprint arXiv:1910.06922*, 2019. [Cited on page 8]
- Kingma, D. P. and Ba, J. Adam: A method for stochastic optimization. *arXiv preprint arXiv:1412.6980*, 2014. [Cited on page 1]

- Korpelevich, G. The extragradient method for finding saddle points and other problems. *Matecon*, 12:747–756, 1976. [Cited on page 8]
- Krizhevsky, A. Learning multiple layers of features from tiny images. Technical report, University of Toronto, 2009. [Cited on page 5]
- Letcher, A., Balduzzi, D., Racaniere, S., Martens, J., Foerster, J. N., Tuyls, K., and Graepel, T. Differentiable game mechanics. *Journal of Machine Learning Research*, 20(84):1–40, 2019. [Cited on pages 6 and 7]
- Liu, M., Mroueh, Y., Ross, J., Zhang, W., Cui, X., Das, P., and Yang, T. Towards better understanding of adaptive gradient algorithms in generative adversarial nets. In *International Conference on Learning Representations*, 2020. URL <https://openreview.net/forum?id=SJxIm0Vtwh>. [Cited on page 8]
- Loizou, N., Berard, H., Jolicoeur-Martineau, A., Vincent, P., Lacoste-Julien, S., and Mitliagkas, I. Stochastic hamiltonian gradient methods for smooth games. In *International Conference on Machine Learning*, pp. 6370–6381. PMLR, 2020. [Cited on page 8]
- Lorraine, J. and Duvenaud, D. Stochastic hyperparameter optimization through hypernetworks. *arXiv preprint arXiv:1802.09419*, 2018. [Cited on page 1]
- Lorraine, J., Vicol, P., and Duvenaud, D. Optimizing millions of hyperparameters by implicit differentiation. In *International Conference on Artificial Intelligence and Statistics*, pp. 1540–1552. PMLR, 2020. [Cited on pages 1 and 8]
- Lucas, J., Sun, S., Zemel, R., and Grosse, R. Aggregated momentum: Stability through passive damping. In *International Conference on Learning Representations*, 2018. [Cited on page 6]
- MacKay, M., Vicol, P., Lorraine, J., Duvenaud, D., and Grosse, R. Self-tuning networks: Bilevel optimization of hyperparameters using structured best-response functions. In *International Conference on Learning Representations (ICLR)*, 2019. [Cited on page 1]
- Maclaurin, D., Duvenaud, D., and Adams, R. Gradient-based hyperparameter optimization through reversible learning. In *International Conference on Machine Learning*, pp. 2113–2122, 2015. [Cited on page 6]
- Maddison, C. J., Paulin, D., Teh, Y. W., O’Donoghue, B., and Doucet, A. Hamiltonian descent methods. *arXiv preprint arXiv:1809.05042*, 2018. [Cited on page 6]
- Mazumdar, E. V., Jordan, M. I., and Sastry, S. S. On finding local Nash equilibria (and only local Nash equilibria) in zero-sum games. *arXiv preprint arXiv:1901.00838*, 2019. [Cited on page 1]
- Mescheder, L., Nowozin, S., and Geiger, A. The numerics of GANs. In *Advances in Neural Information Processing Systems*, pp. 1825–1835, 2017. [Cited on pages 6 and 8]
- Mescheder, L., Geiger, A., and Nowozin, S. Which training methods for gans do actually converge? In *International Conference on Machine Learning (ICML)*, pp. 3481–3490. PMLR, 2018. [Cited on page 8]
- Metz, L., Poole, B., Pfau, D., and Sohl-Dickstein, J. Unrolled generative adversarial networks. *arXiv preprint arXiv:1611.02163*, 2016. [Cited on page 8]
- Morgenstern, O. and Von Neumann, J. *Theory of Games and Economic Behavior*. Princeton University Press, 1953. [Cited on page 1]
- Nagarajan, S. G., Balduzzi, D., and Piliouras, G. From chaos to order: Symmetry and conservation laws in game dynamics. In *International Conference on Machine Learning*, pp. 7186–7196. PMLR, 2020. [Cited on page 7]
- Nesterov, Y. *Introductory lectures on convex optimization: A basic course*, volume 87. Springer Science & Business Media, 2013. [Cited on page 6]
- Nesterov, Y. E. A method for solving the convex programming problem with convergence rate  $o(1/k^2)$ . In *Dokl. Akad. Nauk SSSR*, volume 269, pp. 543–547, 1983. [Cited on pages 1 and 6]
- Nouiehed, M., Sanjabi, M., Huang, T., Lee, J. D., and Razaviyayn, M. Solving a class of non-convex min-max games using iterative first order methods. *Advances in Neural Information Processing Systems*, 32:14934–14942, 2019. [Cited on page 8]
- Omidshafiei, S., Tuyls, K., Czarnecki, W. M., Santos, F. C., Rowland, M., Connor, J., Hennes, D., Muller, P., Pérolat, J., De Vylder, B., et al. Navigating the landscape of multiplayer games. *Nature communications*, 11(1):1–17, 2020. [Cited on page 7]
- Paszke, A., Gross, S., Chintala, S., Chanan, G., Yang, E., DeVito, Z., Lin, Z., Desmaison, A., Antiga, L., and Lerer, A. Automatic differentiation in PyTorch. *Openreview*, 2017. [Cited on page 4]
- Peng, W., Dai, Y.-H., Zhang, H., and Cheng, L. Training gans with centripetal acceleration. *Optimization Methods and Software*, 35(5):955–973, 2020. [Cited on page 8]
- Perolat, J., Munos, R., Lespiau, J.-B., Omidshafiei, S., Rowland, M., Ortega, P., Burch, N., Anthony, T., Balduzzi, D., De Vylder, B., et al. From poincaré recurrence to convergence in imperfect information games:

- Finding equilibrium via regularization. *arXiv preprint arXiv:2002.08456*, 2020. [Cited on page 7]
- Pfau, D. and Vinyals, O. Connecting generative adversarial networks and actor-critic methods. *arXiv preprint arXiv:1610.01945*, 2016. [Cited on page 1]
- Polyak, B. T. Some methods of speeding up the convergence of iteration methods. *USSR Computational Mathematics and Mathematical Physics*, 4(5):1–17, 1964. [Cited on pages 1, 2, 3, 6, and 15]
- Qin, C., Wu, Y., Springenberg, J. T., Brock, A., Donahue, J., Lillicrap, T. P., and Kohli, P. Training generative adversarial networks by solving ordinary differential equations. *arXiv preprint arXiv:2010.15040*, 2020. [Cited on page 8]
- Raghu, A., Raghu, M., Kornblith, S., Duvenaud, D., and Hinton, G. Teaching with commentaries. *arXiv preprint arXiv:2011.03037*, 2020. [Cited on page 1]
- Rajeswaran, A., Mordatch, I., and Kumar, V. A game theoretic framework for model based reinforcement learning. *arXiv preprint arXiv:2004.07804*, 2020. [Cited on page 1]
- Ren, M., Triantafillou, E., Ravi, S., Snell, J., Swersky, K., Tenenbaum, J. B., Larochelle, H., and Zemel, R. S. Meta-learning for semi-supervised few-shot classification. *arXiv preprint arXiv:1803.00676*, 2018. [Cited on page 1]
- Ren, M., Triantafillou, E., Wang, K.-C., Lucas, J., Snell, J., Pitkow, X., Tolias, A. S., and Zemel, R. Flexible few-shot learning with contextual similarity. *arXiv preprint arXiv:2012.05895*, 2020. [Cited on page 1]
- Salimans, T., Goodfellow, I., Zaremba, W., Cheung, V., Radford, A., and Chen, X. Improved techniques for training GANs. In *Advances in Neural Information Processing Systems*, pp. 2234–2242, 2016. [Cited on pages 4 and 13]
- Schäfer, F. and Anandkumar, A. Competitive gradient descent. In *Advances in Neural Information Processing Systems*, pp. 7623–7633, 2019. [Cited on page 6]
- Schäfer, F., Zheng, H., and Anandkumar, A. Implicit competitive regularization in gans. *arXiv preprint arXiv:1910.05852*, 2019. [Cited on page 8]
- Schäfer, F., Anandkumar, A., and Owhadi, H. Competitive mirror descent. *arXiv preprint arXiv:2006.10179*, 2020. [Cited on page 7]
- Sukhbaatar, S., Lin, Z., Kostrikov, I., Synnaeve, G., Szlam, A., and Fergus, R. Intrinsic motivation and automatic curricula via asymmetric self-play. In *International Conference on Learning Representations*, 2018. [Cited on page 1]
- Sutskever, I., Martens, J., Dahl, G., and Hinton, G. On the importance of initialization and momentum in deep learning. In *International Conference on Machine Learning*, pp. 1139–1147, 2013. [Cited on pages 1 and 6]
- Trabelsi, C., Bilaniuk, O., Zhang, Y., Serdyuk, D., Subramanian, S., Santos, J. F., Mehri, S., Rostamzadeh, N., Bengio, Y., and Pal, C. J. Deep complex networks. *arXiv preprint arXiv:1705.09792*, 2017. [Cited on page 1]
- Von Stackelberg, H. *Market Structure and Equilibrium*. Springer Science & Business Media, 2010. [Cited on page 1]
- Wang, Y., Zhang, G., and Ba, J. On solving minimax optimization locally: A follow-the-ridge approach. In *International Conference on Learning Representations*, 2019. [Cited on page 6]
- Wu, Y., Donahue, J., Balduzzi, D., Simonyan, K., and Lillicrap, T. Logan: Latent optimisation for generative adversarial networks. *arXiv preprint arXiv:1912.00953*, 2019. [Cited on page 8]
- Yuan, X., He, P., Zhu, Q., and Li, X. Adversarial examples: Attacks and defenses for deep learning. *IEEE Transactions on Neural Networks and Learning Systems*, 30(9): 2805–2824, 2019. [Cited on page 1]
- Zhang, G. and Yu, Y. Convergence of gradient methods on bilinear zero-sum games. In *International Conference on Learning Representations*, 2019. [Cited on pages 5 and 8]
- Zhang, G., Bao, X., Lessard, L., and Grosse, R. A unified analysis of first-order methods for smooth games via integral quadratic constraints. *arXiv preprint arXiv:2009.11359*, 2020. [Cited on page 8]
- Zhang, J. and Mitliagkas, I. Yellowfin and the art of momentum tuning. *arXiv preprint arXiv:1706.03471*, 2017. [Cited on page 6]
- Zhang, M. R., Lucas, J., Hinton, G., and Ba, J. Lookahead optimizer: k steps forward, 1 step back. *arXiv preprint arXiv:1907.08610*, 2019. [Cited on page 6]

Table 2: Notation

SGD	Stochastic Gradient Descent
SSGD, ASGD	Simultaneous or Alternating SGD
SGDm, SSGDm, ...	... with momentum
GAN	Generative Adversarial Network ( <a href="#">Goodfellow et al., 2014</a> )
IS	Inception Score ( <a href="#">Salimans et al., 2016</a> )
$:=$	Defined to be equal to
$x, y, z, \dots \in \mathbb{C}$	Scalars
$\mathbf{x}, \mathbf{y}, \mathbf{z}, \dots \in \mathbb{C}^n$	Vectors
$\mathbf{X}, \mathbf{Y}, \mathbf{Z}, \dots \in \mathbb{C}^{n \times n}$	Matrices
$\mathbf{X}^\top$	The transpose of matrix $\mathbf{X}$
$\mathbf{I}$	The identity matrix
$\Re(z), \Im(z)$	The real or imaginary component of $z \in \mathbb{C}$
$i$	The imaginary unit. $z \in \mathbb{C} \implies z = \Re(z) + i\Im(z)$
$\bar{z}$	The complex conjugate of $z \in \mathbb{C}$
$ z  := \sqrt{z\bar{z}}$	The magnitude or modulus of $z \in \mathbb{C}$
$\arg(z)$	The argument or phase of $z \in \mathbb{C} \implies z =  z  \exp(i \arg(z))$
$z \in \mathbb{C}$ is <i>almost-positive, almost-negative</i>	$\arg(z) = \pi + \epsilon$ or $\arg(z) = \epsilon$ for small $\epsilon$ respectively
$A, B$	A symbol for the outer/inner players
$d_A, d_B \in \mathbb{N}$	The number of weights for the outer/inner players
$\boldsymbol{\theta}$	A symbol for the parameters or weights of a player
$\boldsymbol{\theta}_A \in \mathbb{R}^{d_A}, \boldsymbol{\theta}_B \in \mathbb{R}^{d_B}$	The outer/inner parameters or weights
$\mathcal{L} : \mathbb{R}^n \rightarrow \mathbb{R}$	A symbol for a loss
$\mathcal{L}_A(\boldsymbol{\theta}_A, \boldsymbol{\theta}_B), \mathcal{L}_B(\boldsymbol{\theta}_A, \boldsymbol{\theta}_B)$	The outer/inner losses $-\mathbb{R}^{d_A+d_B} \mapsto \mathbb{R}$
$\mathbf{g}_A(\boldsymbol{\theta}_A, \boldsymbol{\theta}_B), \mathbf{g}_B(\boldsymbol{\theta}_A, \boldsymbol{\theta}_B)$	Gradient of outer/inner losses w.r.t. their weights in $\mathbb{R}^{d_A/d_B}$
$\boldsymbol{\theta}_B^*(\boldsymbol{\theta}_A) := \arg \min_{\boldsymbol{\theta}_B} \mathcal{L}_B(\boldsymbol{\theta}_A, \boldsymbol{\theta}_B)$	The best-response of the inner player to the outer player
$\mathcal{L}_A^*(\boldsymbol{\theta}_A) := \mathcal{L}_A(\boldsymbol{\theta}_A, \boldsymbol{\theta}_B^*(\boldsymbol{\theta}_A))$	The outer loss with a best-responding inner player
$\boldsymbol{\theta}_A^* := \arg \min_{\boldsymbol{\theta}_A} \mathcal{L}_A^*(\boldsymbol{\theta}_A)$	Outer optimal weights with a best-responding inner player
$d := d_A + d_B$	The combined number of weights for both players
$\boldsymbol{\omega} := [\boldsymbol{\theta}_A, \boldsymbol{\theta}_B] \in \mathbb{R}^d$	A concatenation of the outer/inner weights
$\hat{\mathbf{g}}(\boldsymbol{\omega}) := [\mathbf{g}_A(\boldsymbol{\omega}), \mathbf{g}_B(\boldsymbol{\omega})] \in \mathbb{R}^d$	A concatenation of the outer/inner gradients
$\boldsymbol{\omega}^0 = [\boldsymbol{\theta}_A^0, \boldsymbol{\theta}_B^0] \in \mathbb{R}^d$	The initial parameter values
$j$	An iteration number - fractional values for intermediary steps
$\hat{\mathbf{g}}^j := \hat{\mathbf{g}}(\boldsymbol{\omega}^j) \in \mathbb{R}^d$	The game dynamics - a concatenated gradient at weights $\boldsymbol{\omega}^j$
$\nabla_{\boldsymbol{\omega}} \hat{\mathbf{g}}^j := \nabla_{\boldsymbol{\omega}} \hat{\mathbf{g}} _{\boldsymbol{\omega}^j}$	The Jacobian of the game dynamics $\hat{\mathbf{g}}$ at weights $\boldsymbol{\omega}^j$
$\alpha \in \mathbb{C}$	The step size or learning rate
$\beta \in \mathbb{C}$	The momentum coefficient
$\beta_1 \in \mathbb{C}$	The first momentum parameter for Adam
$\boldsymbol{\mu} \in \mathbb{C}^d$	The momentum buffer
$\lambda \in \mathbb{C}$	Notation for an arbitrary eigenvalue
$\text{Sp}(\mathbf{M}) \in \mathbb{C}^n$	The spectrum – or set of eigenvalues – of $\mathbf{M} \in \mathbb{R}^{n \times n}$
A game is <i>purely adversarial</i> or <i>cooperative</i>	$\text{Sp}(\nabla_{\boldsymbol{\omega}} \hat{\mathbf{g}})$ is purely real or imaginary
A game is <i>partially adversarial</i>	$\text{Sp}(\nabla_{\boldsymbol{\omega}} \hat{\mathbf{g}})$ is neither purely real nor purely imaginary
$\rho(\mathbf{M}) := \max_{z \in \text{Sp}(\mathbf{M})}  z $	The spectral radius in $\mathbb{R}^+$ of $\mathbf{M} \in \mathbb{R}^{n \times n}$
$\mathbf{R} \in \mathbb{R}^{3d \times 3d}$	Augmented dynamics in Corollary 1 - can expand to $\mathbf{R}(\alpha, \beta)$
$\alpha^*, \beta^* := \arg \min_{\alpha, \beta} \rho(\mathbf{R}(\alpha, \beta))$	The optimal step size and momentum coefficient
$\rho^* := \rho(\mathbf{R}(\alpha^*, \beta^*))$	The optimal spectral radius or convergence rate
$\kappa := \frac{\max \text{Sp}(\nabla_{\boldsymbol{\omega}} \mathbf{g})}{\min \text{Sp}(\nabla_{\boldsymbol{\omega}} \mathbf{g})}$	Condition number - defined for convex single-objective optimization
$\sigma_{\min}^2(\mathbf{M}) := \max \text{Sp}(\mathbf{M}^\top \mathbf{M})$	The minimum singular value of a matrix $\mathbf{M}$

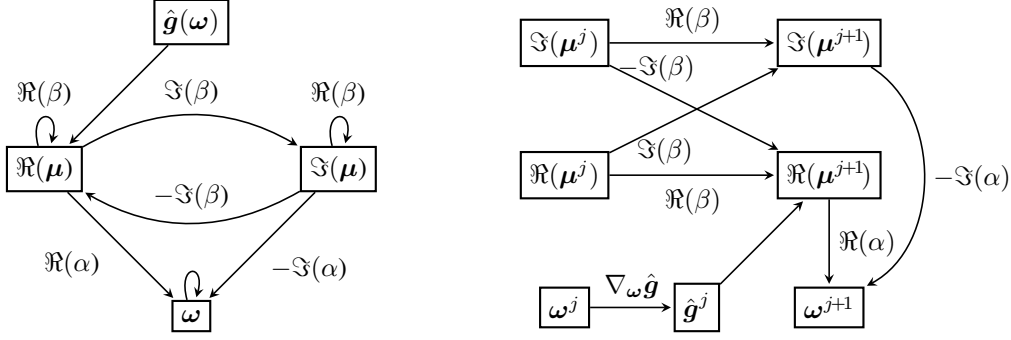


Figure 10: We show two computational diagrams for the simultaneous complex momentum in Algorithm 1. An arrow between nodes indicates that as iterations progress, one value is added to the other scaled by the number over the arrow. No number above an arrow means scaling by 1. Here,  $\mu$  is our momentum buffer,  $\omega$  is a concatenation of the players' parameters,  $\hat{g}(\omega^j) = \hat{g}^j$  is a concatenation of the players' gradients, while  $\alpha$  and  $\beta$  are our step size and momentum coefficients respectively. We show the general case of a complex  $\alpha$ , but we only used a real  $\alpha$  in experiments. *Left:* We emphasize the recurrent link between the real and imaginary components of our momentum buffer  $\Re(\mu)$  and  $\Im(\mu)$ . *Right:* We show the computation in (13), which is key for bounding convergence rates with Theorem 1.

## A. Supporting Results

First, some basic results about complex numbers that are used:

$$z = \Re(z) + i\Im(z) = |z| \exp(i \arg(z)) \quad (21)$$

$$\bar{z} = \Re(z) - i\Im(z) = |z| \exp(-i \arg(z)) \quad (22)$$

$$\exp(iz) + \exp(-iz) = 2 \cos(z) \quad (23)$$

$$\bar{z}_1 \bar{z}_2 = \bar{z}_1 \bar{z}_2 \quad (24)$$

$$1/2(z + \bar{z}) = \Re(z) \quad (25)$$

$$\Re(z_1 z_2) = \Re(z_1)\Re(z_2) - \Im(z_1)\Im(z_2) \quad (26)$$

$$z_1 + z_2 = (\Re(z_1) + \Re(z_2)) + i(\Im(z_1) + \Im(z_2)) \quad (27)$$

$$z_1 z_2 = (\Re(z_1)\Re(z_2) - \Im(z_1)\Im(z_2)) + i(\Im(z_1)\Re(z_2) + \Re(z_1)\Im(z_2)) \quad (28)$$

$$z_1 z_2 = |z_1||z_2| \exp(i(\arg(z_1) + \arg(z_2))) \quad (29)$$

**Lemma 2.**

$$\begin{aligned} \mu^{j+1} &= \beta \mu^j - \hat{g}^j \iff \\ \Re(\mu^{j+1}) &= \Re(\beta)\Re(\mu^j) - \Im(\beta)\Im(\mu^j) - \Re(\hat{g}^j), \Im(\mu^{j+1}) = \Im(\beta)\Re(\mu^j) + \Re(\beta)\Im(\mu^j) - \Im(\hat{g}^j) \end{aligned}$$

*Proof.*

$$\begin{aligned} \mu^{j+1} &= \beta \mu^j - \hat{g}^j \\ \iff \mu^{j+1} &= (\Re(\beta) + i\Im(\beta)) (\Re(\mu^j) + i\Im(\mu^j)) - (\Re(\hat{g}^j) + i\Im(\hat{g}^j)) \\ \iff \mu^{j+1} &= (\Re(\beta)\Re(\mu^j) - \Im(\beta)\Im(\mu^j)) + \\ &\quad i(\Im(\beta)\Re(\mu^j) + \Re(\beta)\Im(\mu^j)) - (\Re(\hat{g}^j) + i\Im(\hat{g}^j)) \\ \iff \mu^{j+1} &= (\Re(\beta)\Re(\mu^j) - \Im(\beta)\Im(\mu^j) - \Re(\hat{g}^j)) + \\ &\quad i(\Im(\beta)\Re(\mu^j) + \Re(\beta)\Im(\mu^j) - \Im(\hat{g}^j)) \\ \iff \Re(\mu^{j+1}) &= \Re(\beta)\Re(\mu^j) - \Im(\beta)\Im(\mu^j) - \Re(\hat{g}^j), \Im(\mu^{j+1}) = \Im(\beta)\Re(\mu^j) + \Re(\beta)\Im(\mu^j) - \Im(\hat{g}^j) \end{aligned}$$

□

We further assume  $\Im(\hat{\mathbf{g}}^j)$  is 0 - i.e., our gradients are real-valued.

**Lemma 3.**

$$\omega^{j+1} = \omega^j + \Re(\alpha \mu^{j+1}) \iff \omega^{j+1} = \omega^j - \Re(\alpha) \hat{\mathbf{g}}^j + \Re(\alpha\beta) \Re(\mu^j) - \Im(\alpha\beta) \Im(\mu^j)$$

*Proof.*

$$\begin{aligned} & \Re(\alpha \mu^{j+1}) \\ &= (\Re(\alpha) \Re(\mu^{j+1}) - \Im(\alpha) \Im(\mu^{j+1})) \\ &= \left( \Re(\alpha) \left( \Re(\beta) \Re(\mu^j) - \Im(\beta) \Im(\mu^j) - \hat{\mathbf{g}}^j \right) - \Im(\alpha) \left( \Im(\beta) \Re(\mu^j) + \Re(\beta) \Im(\mu^j) \right) \right) \\ &= -\Re(\alpha) \hat{\mathbf{g}}^j + \left( \Re(\alpha) \left( \Re(\beta) \Re(\mu^j) - \Im(\beta) \Im(\mu^j) \right) - \Im(\alpha) \left( \Im(\beta) \Re(\mu^j) + \Re(\beta) \Im(\mu^j) \right) \right) \\ &= -\Re(\alpha) \hat{\mathbf{g}}^j + (\Re(\alpha) \Re(\beta) - \Im(\alpha) \Im(\beta)) \Re(\mu^j) - (\Re(\alpha) \Im(\beta) + \Im(\alpha) \Re(\beta)) \Im(\mu^j) \\ &= -\Re(\alpha) \hat{\mathbf{g}}^j + \Re(\alpha\beta) \Re(\mu^j) - \Im(\alpha\beta) \Im(\mu^j) \end{aligned}$$

Thus,

$$\omega^{j+1} = \omega^j + \Re(\alpha \mu^{j+1}) \iff \omega^{j+1} = \omega^j - \Re(\alpha) \hat{\mathbf{g}}^j + \Re(\alpha\beta) \Re(\mu^j) - \Im(\alpha\beta) \Im(\mu^j)$$

□

### A.1. Theorem 1 Proof

**Theorem 1** (Simultaneous Complex Momentum Convergence Rate). *Algorithm 1* with parameters  $\alpha, \beta \in \mathbb{C}$  for games of the form:

$$\mathcal{L}_A(\theta_A, \theta_B) = \theta_A^\top \mathbf{M}_A \theta_B, \mathcal{L}_B(\theta_A, \theta_B) = \theta_A^\top \mathbf{M}_B \theta_B \quad (14)$$

converges linearly with a rate  $\mathcal{O}(\rho(\mathbf{R}) + \epsilon)$ , if the spectral radius  $\rho(\mathbf{R}) < 1$ .

*Proof.* This proof is a simple case of [Polyak \(1964\)](#)'s well-known method for analyzing the convergence of iterative methods. This result can be generalized from quadratic games to when we are sufficiently close to any stationary point  $\omega^*$  with Proposition 4.4.1 from [Bertsekas \(2008\)](#).

For quadratic games, we have that  $\hat{\mathbf{g}}^j = (\nabla_{\omega} \hat{\mathbf{g}})^\top \omega^j$ . Well, by [Lemma 2](#) and [Lemma 3](#) we have:

$$\begin{pmatrix} \Re(\mu^{j+1}) \\ \Im(\mu^{j+1}) \\ \omega^{j+1} \end{pmatrix} = \mathbf{R} \begin{pmatrix} \Re(\mu^j) \\ \Im(\mu^j) \\ \omega^j \end{pmatrix} \quad (30)$$

By telescoping the recurrence for the  $j^{\text{th}}$  augmented parameters:

$$\begin{pmatrix} \Re(\mu^j) \\ \Im(\mu^j) \\ \omega^j \end{pmatrix} = \mathbf{R}^j \begin{pmatrix} \Re(\mu^0) \\ \Im(\mu^0) \\ \omega^0 \end{pmatrix} \quad (31)$$

We can compare  $\mu^j$  with the value it converges to  $\mu^*$  which exists if  $\mathbf{R}$  is contractive. We do the same with  $\omega$ . Because  $\mu^* = \mathbf{R} \mu^* = \mathbf{R}^j \mu^*$ :

$$\begin{pmatrix} \Re(\mu^j) - \Re(\mu^*) \\ \Im(\mu^j) - \Im(\mu^*) \\ \omega^j - \omega^* \end{pmatrix} = \mathbf{R}^j \begin{pmatrix} \Re(\mu^0) - \Re(\mu^*) \\ \Im(\mu^0) - \Im(\mu^*) \\ \omega^0 - \omega^* \end{pmatrix} \quad (32)$$

By taking norms:

$$\left\| \begin{pmatrix} \Re(\boldsymbol{\mu}^j) - \Re(\boldsymbol{\mu}^*) \\ \Im(\boldsymbol{\mu}^j) - \Im(\boldsymbol{\mu}^*) \\ \boldsymbol{\omega}^j - \boldsymbol{\omega}^* \end{pmatrix} \right\|_2 = \left\| \mathbf{R}^j \begin{pmatrix} \Re(\boldsymbol{\mu}^0) - \Re(\boldsymbol{\mu}^*) \\ \Im(\boldsymbol{\mu}^0) - \Im(\boldsymbol{\mu}^*) \\ \boldsymbol{\omega}^0 - \boldsymbol{\omega}^* \end{pmatrix} \right\|_2 \quad (33)$$

$$\implies \left\| \begin{pmatrix} \Re(\boldsymbol{\mu}^j) - \Re(\boldsymbol{\mu}^*) \\ \Im(\boldsymbol{\mu}^j) - \Im(\boldsymbol{\mu}^*) \\ \boldsymbol{\omega}^j - \boldsymbol{\omega}^* \end{pmatrix} \right\|_2 \leq \|\mathbf{R}^j\|_2 \left\| \begin{pmatrix} \Re(\boldsymbol{\mu}^0) - \Re(\boldsymbol{\mu}^*) \\ \Im(\boldsymbol{\mu}^0) - \Im(\boldsymbol{\mu}^*) \\ \boldsymbol{\omega}^0 - \boldsymbol{\omega}^* \end{pmatrix} \right\|_2 \quad (34)$$

With Lemma 11 from Foucart (2012), we have there exists a matrix norm  $\forall \epsilon > 0$  such that:

$$\|\mathbf{R}^j\| \leq (\rho(\mathbf{R}) + \epsilon)^j \quad (35)$$

We also have an equivalence of norms in finite-dimensional spaces. So for all norms  $\|\cdot\|$ ,  $\exists C \geq B > 0$  such that:

$$B\|\mathbf{R}^j\| \leq \|\mathbf{R}^j\|_2 \leq C\|\mathbf{R}^j\| \quad (36)$$

Combining (35) and (36) we have:

$$\left\| \begin{pmatrix} \Re(\boldsymbol{\mu}^j) - \Re(\boldsymbol{\mu}^*) \\ \Im(\boldsymbol{\mu}^j) - \Im(\boldsymbol{\mu}^*) \\ \boldsymbol{\omega}^j - \boldsymbol{\omega}^* \end{pmatrix} \right\|_2 \leq C(\rho(\mathbf{R}) + \epsilon)^j \left\| \begin{pmatrix} \Re(\boldsymbol{\mu}^0) - \Re(\boldsymbol{\mu}^*) \\ \Im(\boldsymbol{\mu}^0) - \Im(\boldsymbol{\mu}^*) \\ \boldsymbol{\omega}^0 - \boldsymbol{\omega}^* \end{pmatrix} \right\|_2 \quad (37)$$

So, we have:

$$\left\| \begin{pmatrix} \Re(\boldsymbol{\mu}^j) - \Re(\boldsymbol{\mu}^*) \\ \Im(\boldsymbol{\mu}^j) - \Im(\boldsymbol{\mu}^*) \\ \boldsymbol{\omega}^j - \boldsymbol{\omega}^* \end{pmatrix} \right\|_2 = \mathcal{O}((\rho(\mathbf{R}) + \epsilon)^j) \quad (38)$$

Thus, we converge linearly with a rate of  $\mathcal{O}(\rho(\mathbf{R}) + \epsilon)$ .  $\square$

## A.2. Characterizing the Augmented Dynamics Eigenvalues

Here, we present polynomials whose roots are the eigenvalues of our augmented dynamics, given the eigenvalues of the Jacobian of the game dynamics  $\text{Sp}(\nabla_{\boldsymbol{\omega}} \hat{g})$ . We use a similar decomposition as Gidel et al. (2019).

We can expand  $\nabla_{\boldsymbol{\omega}} \hat{g} = PTP^{-1}$  where  $T$  is an upper-triangular matrix and  $\lambda_i$  is an eigenvalue of  $\nabla_{\boldsymbol{\omega}} \hat{g}$ .

$$T = \begin{bmatrix} \lambda_1 & * & \dots & * \\ 0 & \dots & \dots & \dots \\ \dots & \dots & \dots & * \\ 0 & \dots & 0 & \lambda_d \end{bmatrix} \quad (39)$$

We then break up into components for each eigenvalue, giving us submatrices  $\mathbf{R}_k \in \mathbb{C}^{3 \times 3}$ :

$$\mathbf{R}_k := \begin{bmatrix} \Re(\beta) & -\Im(\beta) & -\lambda_k \\ \Im(\beta) & \Re(\beta) & 0 \\ \Re(\alpha\beta) & -\Im(\alpha\beta) & 1 - \Re(\alpha)\lambda_k \end{bmatrix} \quad (40)$$

We can get the characteristic polynomial of  $\mathbf{R}_k$  with the following Mathematica command, where we use substitute the symbols  $r + iu = \lambda_k$ ,  $a = \Re(\beta)$ ,  $b = \Im(\beta)$ ,  $c = \Re(\alpha)$ , and  $d = \Im(\alpha)$ .

CharacteristicPolynomial[{{a, -b, -(r + u I)}, {b, a, 0}, {a c - b d, -(b c + a d), 1 - c (r + u I)}}, x]

The command gives us the polynomial associated with eigenvalue  $\lambda_k = r + iu$ :

$$p_k(x) = -a^2x + a^2 + acrx + iacux + 2ax^2 - 2ax - b^2x + b^2 + bdrx + ibdux - crx^2 - icux^2 - x^3 + x^2 \quad (41)$$

Consider the case where  $\lambda_k$  is imaginary – i.e,  $r = 0$  – which is true in all bilinear zero-sum games. Then (41) simplifies to:

$$p_k(x) = -a^2x + a^2 + iacux + 2ax^2 - 2ax - b^2x + b^2 + ibdux - icux^2 - x^3 + x^2 \quad (42)$$



Our complex  $\lambda_k$  come in conjugate pairs where  $\lambda_k = u_k i$  and  $\bar{\lambda}_k = -u_k i$ . (42) has the same roots for  $\lambda_k$  and  $\bar{\lambda}_k$ , which can be verified by writing the roots with the cubic formula. This corresponds to spiraling around the solution in either a clockwise or counterclockwise direction. Thus, we restrict to analyzing  $\lambda_k$  where  $u_k$  is positive without loss of generality.

If we make the step size  $\alpha$  real – i.e.,  $d = 0$  – then (42) simplifies to:

$$p_k(x) = x(-a^2 + iacu - 2a - b^2) + a^2 + x^2(2a - icu + 1) + b^2 - x^3 \quad (43)$$

Using a heuristic from single-objective optimization, we look at making step size proportional to the inverse of the magnitude of eigenvalue  $k$  – i.e.,  $\alpha_k = \frac{\alpha'}{|\lambda_k|} = \frac{\alpha'}{u_k}$ . So, (43) simplifies to:

$$p_k(x) = x(-a^2 + ia\alpha' - 2a - b^2) + a^2 + x^2(2a - i\alpha' + 1) + b^2 - x^3 \quad (44)$$

Notably, in (44) there is no dependence on the components of imaginary eigenvalue  $\lambda_k = r + iu = 0 + iu$ , by selecting a  $\alpha$  that is proportional to its inverse magnitude. We can simplify further with  $a^2 + b^2 = |\beta|^2$ :

$$p_k(x) = x(\Re(\beta)(i\alpha' - 2) - |\beta|^2) + x^2(2\Re(\beta) - i\alpha' + 1) + |\beta|^2 - x^3 \quad (45)$$

We could expand this in polar form for  $\beta$  by noting  $\Re(\beta) = |\beta| \cos(\arg(\beta))$ :

$$p_k(x) = x(|\beta| \cos(\arg(\beta))(i\alpha' - 2) - |\beta|^2) + x^2(2|\beta| \cos(\arg(\beta)) - i\alpha' + 1) + |\beta|^2 - x^3 \quad (46)$$

We can simplify further by considering an imaginary  $\beta$  – i.e.,  $\Re(\beta) = 0$  or  $\cos(\arg(\beta)) = 0$ :

$$p_k(x) = |\beta|^2 - x|\beta|^2 - x^2(i\alpha' - 1) - x^3 \quad (47)$$

The roots of these polynomials can be trivially evaluated numerically or symbolically with the by plugging in  $\beta$ ,  $\alpha$ , and  $\lambda_k$  then using the cubic formula. This section can be easily modified for the eigenvalues of the augmented dynamics for variants of complex momentum by defining the appropriate  $\mathbf{R}$  and modifying the Mathematica command to get the characteristic polynomial for each component, which can be evaluated if it is a sufficiently low degree using known formulas.

### A.3. Convergence Bounds

Suppose we have a bilinear zero-sum game  $\min_{\mathbf{x}} \max_{\mathbf{y}} \mathbf{x}^\top \mathbf{A} \mathbf{y}$  such that  $\text{Sp}(\mathbf{A}^\top \mathbf{A}) \in [\sigma_{min}^2, \sigma_{max}^2]$ . We know from Gidel et al. (2019) that  $\arg(\beta) = \pi$  or  $0$  will not converge for bilinear games with simultaneous updates for any  $\alpha, |\beta|$ . For every  $\arg(\beta)$  that was not  $\pi$  or  $0$  we could select  $\alpha, |\beta|$  to converge by grid-search. However, we could not prove this. Instead, we show there are solutions extremely close to  $\arg(\beta) = \pi$  or  $0$ , and other intermediary values of interest.

For bilinear zero-sum games  $\text{Sp}(\nabla_{\omega} \hat{\mathbf{g}})$  is purely imaginary because  $\nabla_{\omega} \hat{\mathbf{g}}$  is antisymmetric. So,  $\lambda_k \in \text{Sp}(\nabla_{\omega} \hat{\mathbf{g}}) = c_k i$ . Also, eigenvalues occur in conjugate pairs, so  $\lambda_k \in \text{Sp}(\nabla_{\omega} \hat{\mathbf{g}}) = c_k i \implies \exists \bar{\lambda}_k = \text{Sp}(\nabla_{\omega} \hat{\mathbf{g}}) = -c_k i$ . We also have that for  $\mathbf{R}_k$  from (40),  $\text{Sp}(\mathbf{R}_k) = \text{Sp}(\mathbf{R}_{\bar{k}})$ , because (41) is the same for  $\pm c_k$ . So, it suffices to analyze the positive imaginary eigenspaces where  $c_k > 0$ , which we order by their magnitude  $c_k$  – i.e.,  $c_1 \leq c_2 \leq \dots \leq c_n$ .

#### A.3.1. COROLLARY 1 PROOF

**Corollary 1** (Convergence of Complex Momentum). *There exist  $\alpha \in \mathbb{R}, \beta \in \mathbb{C}$  so Algorithm 1 converges for bilinear zero-sum games.*

*Proof.* First, we show that a purely complex  $\beta$  can converge by considering specific fixed choices of  $\alpha, \beta$  that converge for every  $\arg(\beta)$  and eigenspace. For a fixed  $\arg(\beta)$ , in each eigenspace we find a step size that converges, then we select the smallest of those which converges in every eigenspace. The constants in this proof were found with a grid search.

Consider  $\beta = |\beta| \exp(i \arg(\beta)) = 0.7 \exp(i \frac{\pi}{2})$ . The characteristic polynomial from (40) for eigenspace  $k$  is:

$$p(x) = x^2(i\alpha c_k - x + 1) - 0.7^2 x + 0.7^2 \quad (48)$$

Selecting  $\alpha_k = \frac{d}{c_k}$  makes the characteristic polynomial not depend on  $\lambda_k$ . So, this formula for  $\alpha_k$  – with a fixed scale  $d$  – will do the same in each eigenspace. If  $d = 0.7$  then

$$p(x) = x^2(i0.7 - x + 1) - 0.7^2 x + 0.7^2 \quad (49)$$

We can trivially evaluate the roots of  $p(x)$  using the cubic formula. The maximum root size is  $\approx 0.949$ , so we converge in eigenspace  $k$  with this rate. The scale  $d$  and form of  $\alpha_k$  may not be optimal, but they provide a bound. The optimal step size for eigenspace  $k$  may be larger or smaller than  $\alpha_k$ .

Consider  $\hat{\alpha} = \min_k \alpha_k = \min(\frac{0.7}{c_k})$ . We know  $\alpha_k$  converges in eigenspace  $k$  with a rate of  $\approx 0.949$ , and  $0 < \hat{\alpha} \leq \alpha_k$ . So,  $\hat{\alpha}$  also converges in eigenspace  $k$ , which is less than or equal to a step size which converges in each eigenspace and greater than 0, so it converges in each eigenspace.  $\square$

### A.3.2. COROLLARY 2 PROOF

**Corollary 2** (Almost-real Momentum can Converge). *For small  $\epsilon$  (we show for  $\epsilon = \frac{\pi}{16}$ ), if  $\arg(\beta) = \pi - \epsilon$  (i.e., almost-negative) or  $\arg(\beta) = \epsilon$  (i.e., almost-positive), then we can select  $\alpha, |\beta|$  so Algorithm 1 converges on bilinear zero-sum games.*

*Proof.* We repeat the logic in section A.3.1 for  $\arg(\beta)$  that are almost-real – i.e., close to  $\pi$  or 0. The constants in this proof were found with a grid search.

First, consider  $\arg(\beta) = \pi - \epsilon = \pi - \frac{\pi}{16}$  with  $\alpha_k = \frac{0.75}{c_k}$  and  $|\beta| = 0.986$ . Using the cubic formula on the associated  $p(x)$  from (41) the maximum magnitude root has size  $\approx 0.9998$ . So, selecting  $\hat{\alpha} = \min_k \alpha_k$  will converge in each eigenspace.

Now, consider  $\arg(\beta) = \epsilon = \frac{\pi}{16}$  with  $\alpha_k = \frac{0.02}{c_k}$  and  $|\beta| = 0.9$ . Using the cubic formula on the associated  $p(x)$  from (41) the maximum magnitude root has size  $\approx 0.9865$ . Again, selecting  $\hat{\alpha} = \min_k \alpha_k$  will converge in each eigenspace.  $\square$

## B. Algorithms

Here, we include additional algorithms, which may be of use to some readers. Algorithm 4 shows our method with all real-valued objects, if one wants to implement complex momentum in a library that does not support complex arithmetic.

---

### Algorithm 3 (Alt) Momentum

---

```

1:  $\beta \in \mathbb{C}, \alpha \in \mathbb{R}^+$ 
2: for  $i = 1 \dots N$  do
3:    $\mu_A^{j+1} = \beta \mu_A^j - g_A^j$ 
4:    $\theta_A^{j+1} = \theta_A^j + \Re(\alpha \mu_A^{j+1})$ 
5:    $\mu_B^{j+1} = \beta \mu_B^j - g_B(\theta_A^{j+1}, \theta_B^j)$ 
6:    $\theta_B^{j+1} = \theta_B^j + \Re(\alpha \mu_B^{j+1})$ 
return  $\omega_N$ 

```

---



---

### Algorithm 4 Simultaneous Complex Momentum - $\mathbb{R}$ valued

---

```

1:  $\Re(\beta), \Im(\beta), \Re(\alpha), \Im(\alpha) \in \mathbb{R}$ 
2: for  $j = 1 \dots N$  do
3:    $\Re(\mu^{j+1}) = \Re(\beta)\Re(\mu^j) - \Im(\beta)\Im(\mu^j) - \hat{g}^j$ 
4:    $\Im(\mu^{j+1}) = \Re(\beta)\Im(\mu^j) + \Im(\beta)\Re(\mu^j)$ 
5:    $\omega^{j+1} = \omega^j - \Re(\alpha)\hat{g}^j + \Re(\alpha\beta)\Re(\mu^j) - \Im(\alpha\beta)\Im(\mu^j)$ 
return  $\omega_N$ 

```

---

### B.1. Complex Momentum in PyTorch

Our method can be easily implemented in PyTorch 1.6+ by using complex tensors. The only necessary change to the SGD with momentum optimizer is extracting the real-component from momentum buffer as with Jax – see [here](#).

In older versions of Pytorch, we can use a tensor to represent the momentum buffer  $\mu$ , step size  $\alpha$ , and momentum coefficient  $\beta$ . Specifically, we represent the real and imaginary components of the complex number independently. Then, we redefine the operations `__add__` and `__mult__` to satisfy the rules of complex arithmetic – i.e., equations (27) and (28).

## C. Experiments

### C.1. Computing Infrastructure and Runtime

For the bilinear zero-sum experiments in Sections 4.1 and 4.2, we do our computing in CPU. Training each 2-D GAN in Section 4.3 takes 2 hours and we can train 10 simultaneously on an NVIDIA T4 GPU. Training each CIFAR GAN in Section 4.4 takes 10 hours and we can only train 1 model per NVIDIA T4 GPU.

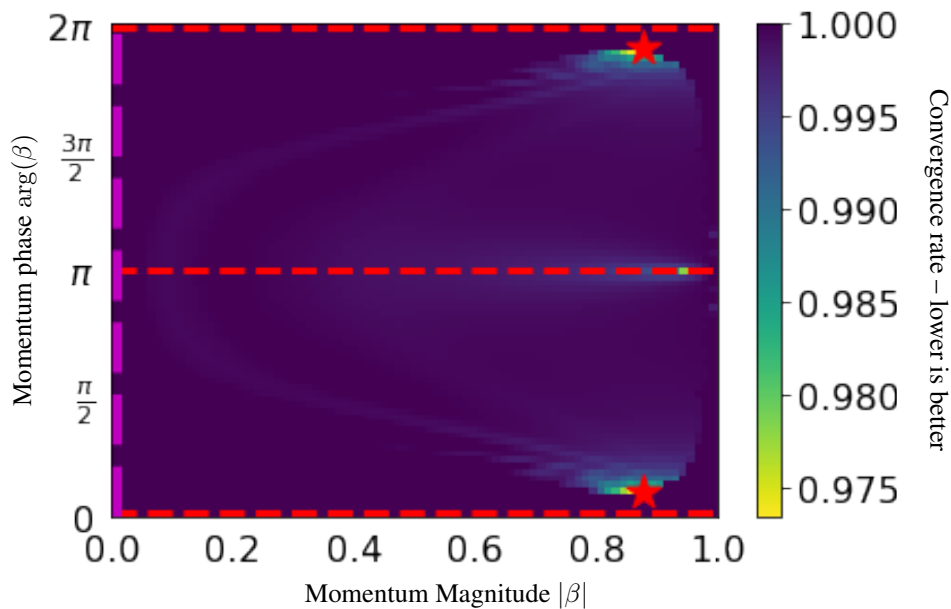


Figure 11: Convergence rates for alternating complex momentum on  $\min_x \max_y xy$ . The step size is fixed to  $\alpha = 0.1$ , while we vary the phase and magnitude of the complex momentum  $\beta = |\beta| \exp(i \arg(\beta))$ . There is a red star the optima, dashed red lines at real  $\beta$ , and a dashed magenta line for alternating gradient descent. The results are symmetric about  $\arg(\beta) = \pi$ . This is the alternating update variant of Figure 2. Negative momentum can converge here, as shown by Gidel et al. (2019).

## C.2. Optimization in Bilinear Zero-Sum Games

We include the alternating update version of Figure 2 in Figure 11. With alternating updates on bilinear zero-sum games for  $\alpha = 0.1$  the best value we found for the momentum coefficient  $\beta$  was complex, but we could converge with real, negative momentum. When results diverge for Figures 2 and 11, we clip the convergence rate to display 1.0.

## C.3. Spectrum of the Augmented Dynamics

We include Figure 12 which investigates a GANs spectrum throughout training, and elaborates on the information that is shown in Figure 9. This shows that there are many real and imaginary eigenvalues, so GAN training can be partially adversarial. Also, the structure of the set of eigenvalues for the discriminator is different than the generator, which may motivate separate optimizer choices. The structure between the players persists through training, but the eigenvalues grow in magnitude and spread out their phases. This indicates how adversarial the game is may change during training.

## C.4. Training GANs on 2-Dimensional Distributions

For 2-D distributions, the data is generated by sampling from a mixture of 8 Gaussian distributions, which are distributed uniformly around the unit circle.

For the GAN, we use a fully-connected network with 4 hidden ReLU (Hahnloser et al., 2000) layers with 256 hidden units. We chose this architecture to be the same as Gidel et al. (2019). Our noise source for the generator is a 4-D Gaussian. We trained the models for 100 000 iterations. The performance of the optimizer settings is evaluated by computing the negative log-likelihood of a batch of 100 000 generated 2-D samples.

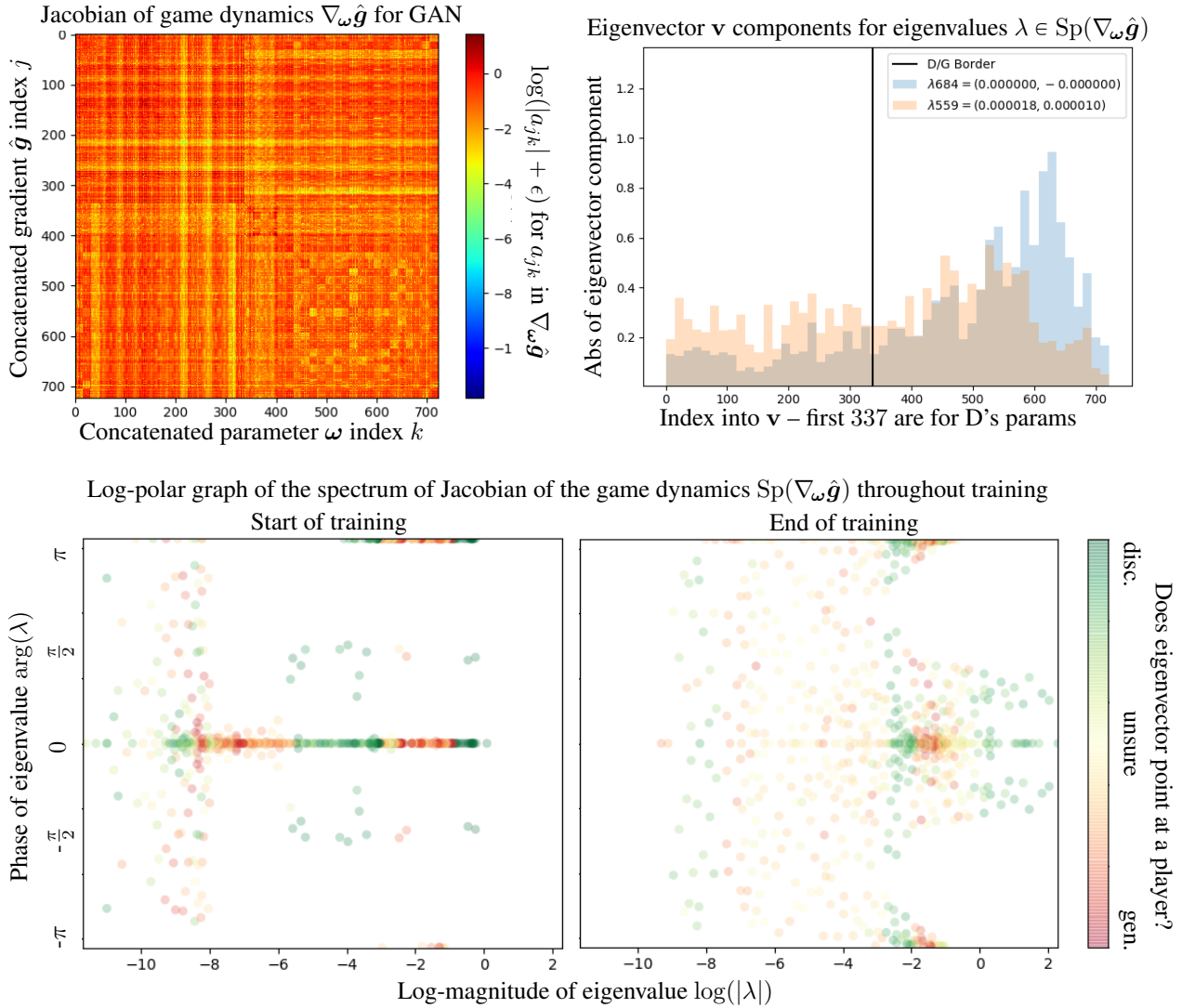


Figure 12: These plots investigate the spectrum of the Jacobian of the game dynamics for the GAN in Figure 9 through training. The spectrum is key for bounding convergence rates in learning algorithms.

*Top left:* The Jacobian  $\nabla_{\omega} \hat{g}$  for a GAN on a 2-D mixture of Gaussians with a two-layer, fully-connected 16 hidden unit discriminator (D) and generator (G) at the end of training. In the concatenated parameters  $\omega \in \mathbb{R}^{723}$ , the first 337 are for D, while the last 386 are for G. We display the log of the absolute value of each component plus  $\epsilon = 10^{-10}$ . The upper left and lower right quadrants are the Hessian of D and G's losses respectively.

*Top Right:* We visualize two randomly sampled eigenvectors from  $\nabla_{\omega} \hat{g}$ . The first part of the parameters is for the discriminator, while the second part is for the generator. Given an eigenvalue with eigenvector  $\mathbf{v}$ , we roughly approximate attributing eigenvectors to players by calculating how much of it lies in D's parameter space with  $\frac{\|\mathbf{v}_{1:337}\|_1}{\|\mathbf{v}\|_1} = \frac{\|\mathbf{v}_{1:337}\|_1}{\|\mathbf{v}\|_1}$ . If this ratio is near 1 (or 0) and say *the eigenvector mostly points at D (or G)*. The blue eigenvector mostly points at G, while the orange eigenvector is unclear. Finding useful ways to attribute eigenvalues to players is an open problem.

*Bottom:* The spectrum of the Jacobian of the game dynamics  $\text{Sp}(\nabla_{\omega} \hat{g})$  is shown in log-polar coordinates, because it is difficult to see structure when graphing in Cartesian (i.e.,  $\Re$  and  $\Im$ ) coordinates, due to eigenvalues spanning orders of magnitude, while being positive and negative. The end of training is when we stop making progress on the log-likelihood. We have imaginary eigenvalues at  $\arg(\lambda) = \pm\pi/2$ , positive eigenvalues at  $\arg(\lambda) = 0$ , and negative eigenvalues at  $\arg(\lambda) = \pm\pi$ .

*Takeaway:* There is a banded structure for the coloring of the eigenvalues that persists through training. We may want different optimizer parameters for the discriminator and generator, due to asymmetry in their associated eigenvalues. Also, the magnitude of the eigenvalues grows during training, and the args spread out indicating the game may change how adversarial it is near solutions.

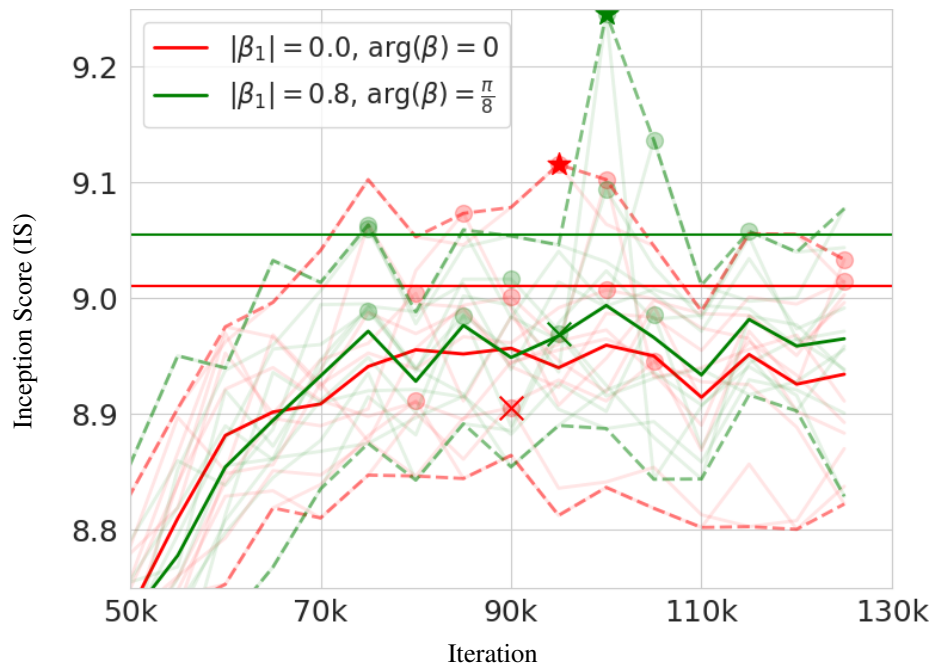


Figure 13: We compare the best optimization parameters from grid-search Figure 6 for our complex Adam variant (i.e., Algorithm 2) shown in green, with the author provided values shown in red for the CIFAR-10 BigGAN over 10 seeds. A star is displayed at the best IS over all runs, a cross is displayed at the worst IS over all runs, while a circle is shown at the best IS for each run. Dashed lines are shown at the max/min IS over all runs at each iteration, low-alpha lines are shown for each runs IS, while solid lines are shown for the average IS over all seeds at each iteration. The results are summarized in Table 1.